ADVANCED ENERGY MATERIALS
www.advenergymat.de

Advancing Energy Materials by In Situ Atomic Scale Methods

Christian Jooss, Michael Seibt,* Martin Wenderoth, Oliver Bünermann, Ole Bunjes, Till Domröse, Christian Eckel, Francesca Falorsi, Christoph Flathmann, Monica Kolek Martinez de Azagra, Matthias Krüger, Jonas Lindner, Tobias Meyer, Claus Ropers, Ulrich Ross, Kai Rossnagel, Sreeju Sreekantan Nair Lalithambika, Simone Techert, Georg A. Traeger, Cynthia Volkert, R. Thomas Weitz, and Alec M. Wodtke*

Despite significant advancements in materials design for renewable energy devices, the fundamental understanding of the underlying processes in many materials remains limited, particularly in complex, inhomogeneous systems and interfaces. In such cases, in situ studies with high spatial and energy resolution are essential for uncovering new insights into excitation, dissipation, and conversion processes. Recent progress in in situ atomic scale methods has greatly enhanced the understanding of energy materials. Here, key advances are reviewed, including in situ, environmental and ultra-fast transmission electron microscopy, scanning probe techniques, single-photon-resolved infrared spectroscopy, velocity-resolved molecular kinetics, and in situ grazing-incidence X-ray spectroscopy. These techniques enable the study of energy conversion with spatial resolution from nanometers down to individual atoms, energy resolution down to meV, and single-quantum detection. Especially they enable access to processes that involve multiple degrees of freedom, strong coupling, or spatial inhomogeneities. They have driven a qualitative leap in the fundamental understanding of energy conversion processes, opening new avenues for improving existing materials and designing novel clean and efficient energy materials in photovoltaics, friction, and surface chemistry and (photo-)electrochemistry.

1. Introduction

Driven by worldwide ecological and economic needs to replace fossil energy sources, tremendous efforts in science and technology have been undertaken to advance renewable energy harvesting. Remarkable progress has already been achieved in various fields, such as in silicon-based photovoltaics,[1] electrolysis,[2] catalytic conversion,[3] or reduction of friction losses,[4] although virtually all technologies still show performances much below fundamental theoretical limits. In fact, the need of fundamental research on energy conversion processes has been identified as one of the key research fields in condensed matter physics quite some time ago.[5] The overarching goal of such research is to ultimately understand and control energy conversion processes in materials down to the atomic and quantum levels. A substantial part of these

C. Jooss, J. Lindner, T. Meyer, U. Ross, C. Volkert
Institute of Materials Physics
University of Goettingen
Friedrich-Hund-Platz 1, 37077 Goettingen, Germany
E-mail: jooss@ump.gwdg.de

C. Jooss, O. Bünermann, C. Ropers, C. Volkert, R. T. Weitz, A. M. Wodtke
International Center for Advanced Studies of Energy Conversion (ICASEC)
Tammannstr. 6, 37077 Goettingen, Germany

The ORCID identification number(s) for the author(s) of this article can be found under https://doi.org/10.1002/aenm.202404280

DOI: 10.1002/aenm.202404280

M. Seibt, M. Wenderoth, O. Bunjes, T. Domröse, C. Flathmann, C. Ropers, U. Ross, G. A. Traeger
4th Institute of Physics
University of Goettingen
Friedrich-Hund-Platz 1, 37077 Goettingen, Germany
E-mail: michael.seibt@uni-goettingen.de

O. Bünermann, A. M. Wodtke
Institute of Physical Chemistry
University of Goettingen
Tammannstr. 6, 37077 Goettingen, Germany

T. Domröse, C. Ropers
Department of Ultrafast Dynamics
Max Planck Institute for Multidisciplinary Sciences
Am Faßberg 11, 37077 Goettingen, Germany

C. Eckel, F. Falorsi, M. K. M. de Azagra, R. T. Weitz
1st Institute of Physics
University of Goettingen
Friedrich-Hund-Platz 1, 37077 Goettingen, Germany

processes occurs at interfaces including surfaces. Examples include breaking up or formation of chemical bonds at surfaces or in Helmholtz layers, charge transfer and separation at interfaces, energy dissipation in sliding systems, or quasi-particle formation at phase boundaries evolving in phase transitions.

Clearly, such locally confined or spatially inhomogeneous processes need to be studied by experimental methods that offer sufficiently high spatial resolution, i.e., typically at the nanometer range down to atomic scales. Furthermore, high energy resolution down to meV and single quantum detection capabilities are required in order to distinguish contributions from different processes to energy conversion or to achieve chemical selectivity. Common to all energy conversion processes is their inherent non-equilibrium nature. Hence, it is mandatory to study structural and electronic properties during the course of energy conversion, rather than prior to and subsequent to such process, in other words, suitable high-resolution methods have to work *operando* or in situ rather than *post mortem*.

This review provides overview on current progress of experimental in situ studies of energy conversion processes that enabled the involved processes to be studied at high spatial resolution. This has required further development of appropriate experimental (and theoretical) tools, often initially related to the study of a specific material problem, and then providing a basis for their more general application to studies of a wide class of problems. It is therefore natural to present the methodological developments exemplified by some representative examples of the investigation of new and advanced energy materials, which are often still in the stage of basic research.

As outlined above, the topic involves a rather broad area of scientific questions in physics, chemistry, and materials sciences, thus requiring a rather broad scope of this overview. Clearly, such overview cannot be complete. Our focus is on experimental studies. Seeking for comprehensive understanding down to atomic scales and quantum level is guiding the choice of examples suitable to demonstrate the achieved progress with the overarching theme of methods for investigating surface and interface processes.

Our review is thus organized as follows:

Chapter 2: Interfaces in photovoltaics down to atomic scales. Interfaces of various kinds – including surfaces – are essential parts of devices for photovoltaic energy conversion. As the most familiar example, p-n homojunctions facilitate excess charge carrier separation due to their intrinsic electric field at interfaces. Along this line, there are systems with increasing complexity such as p-n heterojunctions,[6] halide perovskites,[7] or systems with carrier-selective contacts.[8] The experimental study of physical properties such as band discontinuities, space charge layers, charge recombination and separation as well as charge dynamics at dopants and their interconnection to structure requires in situ atomic scale methods. This is especially true for materials constituting strongly correlated electron-phonon systems, where the interface transfer is associated with a change in the fundamental character of charge carriers.[9,10]

Recent years have witnessed astonishing progress in (scanning) transmission electron microscopy, (S)TEM, techniques targeting at in situ characterization of such interfaces (or junctions) down to atomic column resolution.[11,12] Techniques summarized in this review include electric field mapping at interfaces using *momentum resolved STEM* (MRSTEM), *electron beam induced current in STEM* (STEM-EBIC) capable to map currents of semiconductor (Si, GaAs) and oxide (manganite, titanites) junctions and hence – in combination with quantitative simulations – provide information about recombination-active defects and junction properties under applied external voltage. In addition, a technique suitable to measure the electron affinity at junctions by evaluating the *near-edge structure* of the O_K core loss edge in *EELS* spectra obtained in perovskite metal oxides will be described.

Recent developments in scanning tunneling microscopy (STM) and related spectroscopy (STP) provide insight into the electronic structure of dopants in semiconductors in their ground state and – in particular – in their excited states as well as their change close to interfaces with atomic-scale spatial resolution.[13,14] The successful combination of STM with time-resolved near-field optical excitation makes it possible to investigate individual donor sites at different distances from the semiconductor surface showing a significant variation in the lifetime of a nanoscopic system.

Chapter 3: Atomic processes in dissipation and friction at surfaces. Energy conversion is inevitably connected to energy losses, where energy flows into undesired dissipative channels. In particular, the identification of energy dissipation pathways involved in forming or breaking chemical bonds on surfaces, a central question for steering catalytic activity, requires well-defined atomic scale and quantum-level studies.[15] Determining the energy and angle distribution of scattered atoms by velocity-resolved kinetic methods is one of the most direct experimental probes of the dynamics of gas phase molecular collision processes at surfaces.[16] Using laser-based atom tagging,[17] such measurements have been developed toward a versatile tool to identify processes of interaction of individual atoms and molecules with surfaces of metals, semiconductors, and insulators in combination with advanced theoretical calculations. This offers exciting new insights into the atomic and quantum

M. Krüger
Institute for Theoretical Physics
University of Goettingen
Friedrich-Hund-Platz 1, 37077 Goettingen, Germany
K. Rossnagel
Ruprecht Haensel Laboratory
Deutsches Elektronen-Synchrotron DESY
Notkestr. 85, 22607 Hamburg, Germany
K. Rossnagel
Institute of Experimental and Applied Physics
Kiel University
Olshausenstr. 40, 24098 Kiel, Germany
S. S. N. Lalithambika, S. Techert
FS Structural Dynamics in Chemical Systems
Deutsches Elektronen-Synchrotron DESY
Notkestr. 85, 22607 Hamburg, Germany
S. Techert
Institute for X-Ray Physics
University of Goettingen
Friedrich-Hund-Platz 1, 37077 Goettingen, Germany
A. M. Wodtke
Department of Dynamics at Surfaces
Max Planck Institute for Multidisciplinary Sciences
Am Faßberg 11, 37077 Goettingen, Germany

mechanism of energy transfer that results in bond making and breaking at surfaces.

There has been huge progress in studying and understanding friction of sliding contacts beyond empirical laws of energy dissipation.[18] However, understanding of atomic scale mechanisms has required studies distinguishing different microscopic dissipation channels. Atomic scale studies have become possible by atomic force microscopy (AFM) with well-controlled tips and environments. They allowed for shedding light onto the role of electron, phonon, and other structural degrees of freedom at surfaces and in sub-surface layers. This includes an understanding of quantum effects such as electron-phonon coupling including the effect of polaron formation in surface dissipation in oxide and multilayer thin films.

Chapter 4: Nanoscale studies of phase transitions in energy materials. Phase transitions in energy materials can be either induced by temperature changes, external fields, or due to sufficiently strong excitations that can occur in operation.[19,20] The resulting change in atomic and electronic structure can have a strong influence on energy conversion processes. While on the one hand, phase transitions offer new degrees of freedom for controlling excitation and energy conversion, on the other hand, the emergence of new quasiparticles and/or the formation of new structural inhomogeneities, such as defects or phase boundaries demand new in-depth analytical tools down to the atomic level in order to decipher such complex scenarios and the interplay of an unknown number of parameters. An important class of examples are optically driven phase transitions on surfaces that can be excellently studied in 2D materials[21] such as 1T-TaS_2. Furthermore, spatiotemporal inhomogeneity evolves at phase transitions in transition metal perovskite oxides.[22]

To address all these questions, in situ and operando methods capable to study phase transformations at high spatial resolution are required to understand how they steer energy conversion processes. The development of in situ transmission electron microscopy (TEM) allowed to get insight into structural changes during phase transitions of nano-scale materials including metastable transient states that are not present in the bulk and require atomistic information.[23] Furthermore, scanning probe methods like scanning nearfield optical Microscopy (SNOM) enable to study optical and electronic fingerprints of phase transitions including nanodomain formation with high spatial resolution,[24] whereas scanning tunneling microscopy (STM) reveals related surface information. Finally, the capability of studying spatiotemporal dynamics by using electron scattering and diffraction in ultrafast setups such as ultrafast low-energy electron diffraction (ULEED) and ultrafast transmission electron microscopy (UTEM) has been developed and contributed to the understanding of the transformation of energy and materials.[25]

Chapter 5: Atomic scale and quantum studies of dynamic interfaces in reactive states. Interfaces are the most relevant sites, where chemical reactions take place and can be controlled. In particular, aqueous and gaseous interfaces are extremely important for catalysis and electro- or photochemical processes.[26] A comprehensive understanding of the atomic and quantum dynamics at interfaces during chemical conversion is required. A prominent example is the atomic and electronic structure of the electric double layer, where atomic resolution studies are required in addition to the enormous recent progress in modeling by ab initio molecular dynamics.[27] This also involves topics of coordination chemistry and active sites in catalysis.[28]

In order to study such phenomena, in situ techniques that allow high spatial and energy resolution in controllable reactive conditions are required. Grazing incidence in situ x-ray spectroscopy techniques have been developed to a level to provide insights into the change of coordination of reactive sites, for example at interfaces of complex oxides to water.[29] Complementarily, the development of high-resolution aberration-corrected TEM under environmental conditions (ETEM) offers unprecedented real-space information about reactive states of surfaces.[30] The latter is currently advancing into a quantitative technique for studying cooperative dynamics on surfaces during reactions as the result of aberration-corrected electron optics and sensitive cameras in combination with recent progress in the control of electrochemical conditions of electron transparent electrodes.[31,32] In particular, electron holography techniques have been driven to atomic resolution in ETEM setups thus providing fresh insights into the atomic and electronic structure of reactive interfaces, including the structure and dynamics of the electric double layer.

For the study of catalytic surfaces under ambient conditions, scanning tunneling microscopy (STM) has been developed as a versatile tool with atomic resolution. It can be operated in the full pressure range from ultra-high vacuum (UHV) to 1 bar, where behavior at high gas pressures is often different than a mere extrapolation of low-pressure studies.[33] Progress includes to overcome experimental challenges like image stability caused by drift or additional noise due to pressure variations.[34] The combination of in situ STM with in situ X-ray spectroscopy has allowed to uncover the correlation of gas-induced change of surface atomic structure with carbon dioxide (CO_2) activation pathways.[35]

Furthermore, the effect of vibrational excitations and energy flow on chemical dynamics is hardly understood and needs to be addressed.[36] This requires methods that can study vibrational energy on a quantum level. Recent developments of single photon infrared spectroscopy opened a window for studying quantum effects in chemical energy conversion.[37]

Chapter 6 summarizes the main advances made by atomic and quantum-level methods and addresses some of the key open challenges that need to be solved to further advance the understanding of complex energy materials at the atomic level.

2. Photovoltaics Down to Atomic Scales: Space Charge Layers, Band Discontinuities, Charge Carrier Recombination and Separation, Dopants

Third-generation photovoltaics aims at ultrahigh efficiency beyond the Shockley-Queisser limit[38] serving as the detailed-balance benchmark for single junction solar cells. A straightforward approach is the multijunction solar cell technology[39] reducing transmission as well as thermalization losses. In addition, a plethora of schemes have been proposed[40,41] whose realization requires fundamental understanding of the atomic, chemical, and electronic structure of materials and their interfaces from the atomic to the nanometer scale.

Figure 1 illustrates important length scales (indicated by Λ) and quantities for the example of a p-n heterojunction: (a) Typical bulk quantities ($\Lambda = \infty$) such as conduction band (E_{Cn}, E_{Cp})

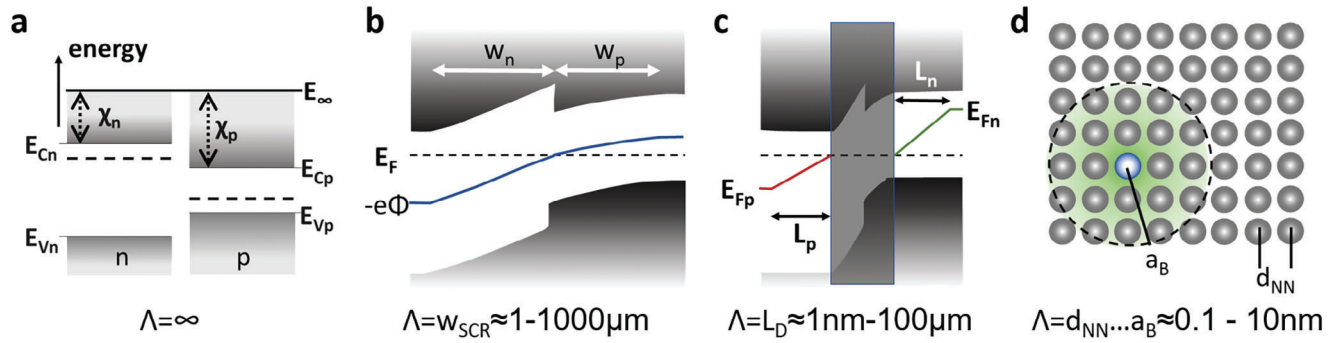

Figure 1. Relevant length scales (Λ) and quantities of a p-n heterojunction. a) E∞: vacuum level, $\chi_{n,p}$: electron affinities, $\Phi_{n,p}$: work functions, $E_{Vn,p}$ and $E_{Cn,p}$: valence and conduction band edges, respectively, dashed lines indicate Fermi levels. b) Gradients of quasi-Fermi levels driving excess carrier diffusion described by diffusion lengths L_n and L_p. c) Electric potential within the space charge region (SCR) of width $w_{SCR}=w_n+w_p$. d) Charge dynamics of dopant atoms at interfaces and surfaces (for details, see text).

and valence band edges (E_{Vn}, E_{Vp}) on the energy scale defined by the vacuum level E_∞ and the electron affinities (χ_n and χ_p). They all require some re-consideration at interfaces in general and at "real" – not atomically sharp – interfaces in particular. In Section 2.1, we review the spatially resolved measurement of band gap energy and electron affinity using electron energy loss spectroscopy (EELS), allowing a spatial resolution in the sub-nm range. Figure 1b: Electric fields at junctions are essential for carrier separation and transport toward external contacts. Clearly, their length scale is determined by the space charge region width and hence mainly by the doping levels of the constituting materials varying from the µm – for low doping – down to the nanometer range for high doping concentrations. Again, measuring magnitude and spatial profiles is essential to understand the junction behavior and requires high spatial resolution. In Section 2.2, electron holography (EH) and momentum resolved scanning TEM (MRSTEM) techniques are discussed that allow a spatial resolution from 100′s down to the sub-nm range. Figure 1c: An essential process for photovoltaic energy conversion is excess carrier diffusion from the neutral absorber material to the selective contacts whose length scale spans from several hundred microns in high-efficiency Si solar cells down to the nanometer range in complex materials.[42,43] This requires high-resolution techniques reaching spatial resolution beyond 1 µm typical for standard optical techniques.[44] In Section 2.3, we discuss the measurement of junction currents and related bulk diffusion lengths using scanning electron beam-induced current (STEM-EBIC) now having been developed to Angstrom spatial resolution in transmission electron microscopes.

Figure 1d sketches the environment of a single dopant atom in a semiconductor indicating relevant length scales such as the atomic distance (d_{NN}≈0.1 nm) and the extension of donor wavefunctions estimated by their Bohr radius (a_B≈1–10 nm). In particular, in complex and numerous new materials, mechanisms determining these non-equilibrium properties and the local impact of the interface atomic structure interfaces or of other defects are not well understood. Thus, in situ methods that are able to correlate diffusion length, electric fields, or donor activity to the atomic structure of the devices are highly desirable. We consider the analysis of electronic structure and dynamics of dopants by STM and related spectroscopy (STP) on the atomic scale in S2.4.

2.1. Study of Band Discontinuities at Heterojunctions Using High Resolution Electron Energy Loss Spectroscopy (EELS)

Understanding of properties of heterojunctions often requires atomic scale information.[45] For this purpose, atomic scale information on bandgap energies and band discontinuities, encoded in the electron affinity, is required. In principle, the low energy part of EEL spectra, subsequently referred to as valence EELS (VEELS), contains information about the energy of the band gap as the lowest available empty states. Typical loss spectra in the VEELS regime, however, contain contributions from phonon and plasmon excitations[46] and from Cherenkov radiation,[47] which is especially prominent in semiconductors with their rather large permittivity and hence large refractive index. Nevertheless, in combination with simulations of VEEL spectra, spatial band gap energy variations in the range of 0.1 eV can be distinguished and mapped on a sub-nanometer scale.[48] Simultaneous acquisition of core-loss EELS and VEELS by using a dual-EELS system or by simultaneous EDX mapping allows to correlate the exact composition of the material in every location with the electronic structure. We also note that the problems with plasmon and Cherenkov artefacts may at least partly be solved by the emerging technique of momentum resolved EELS[49] and simulation of EEL spectra.

Core-loss EELS under suitable conditions can be used to measure local variations in electron affinity across materials and interfaces.[50] The EELS intensity, in dipole approximation, is proportional to the overlap of the initial and final state wavefunctions times the density of states (DOS).[51] To measure the local variation in electron affinity, an electronic transition from a core level to the lowest unoccupied states is chosen, and the energy of the corresponding EELS peak is measured as a function of position. Since the core level is practically unaffected by bonding, its energy remains unchanged with respect to the vacuum level, while the energy of the unoccupied states changes with the local bonding conditions. Hence, the changes of the energy of the EELS peak at different positions are the inverse of the change of the electron affinity. However, as EELS always measures the energy difference between a core state and a final state in the presence of a core hole, this simple interpretation is only possible if these many-particle effects are either negligible or corrected.[51] Nevertheless, the method has successfully been applied in

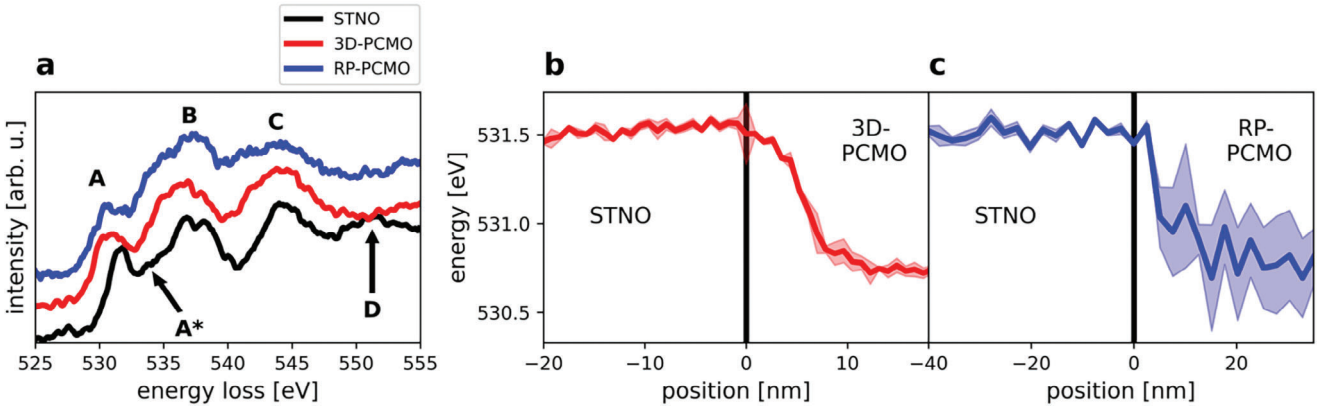

Figure 2. Band offsets determined by EELS of the O K-edge. a) shows EEL spectra of the O K-edge with labels to the characteristic peaks for three different materials. b) and c) show the energy shift of peak A across an STNO/3D-PCMO and an STNO/RP-PCMO junction. Reproduced under terms of the CC-BY license,[45] © 2023, The Author, published by eDiss-SUB Göttingen.

literature, as, e.g., Saucke et al. have measured the change of the local electron affinity across a heterojunction of niobium-doped strontium titanate (STNO) and praseodymium calcium manganite (PCMO) at different temperatures.[50] Such manganites represent hot polaron absorbers and are studied in order to develop a fundamental understanding of hot carrier stabilization mechanisms in strongly correlated electron systems.[42,52] Saucke and co-workers[50] found a difference in the materials' electron affinities of $\chi = 0.65(4)$ eV to 0.57(5) eV at temperatures of $T = 300$ and 80K, respectively, resulting in a conduction band offset. We used this method to quantify the changes in electron affinity across an STNO/PCMO and an STNO/RP-PCMO junction. As shown in **Figure 2**a), the onset of the O K-edge (peak A), corresponding to the lowest unoccupied states, shifts depending on the material. Tracking this onset, we found a difference in electron affinities across the junction of $\chi = 0.8(5)$ eV for both heterojunctions. Furthermore, Figure 2b,c reveals that the electron affinities change over a transition region of roughly 10 nm at the interface due to intermixing.[45] Measuring the local electron affinity with EELS requires (i) negligible by core hole effects and (ii) the existence of a reference state as a common chemical species on both sides of the interface (such as oxygen in our case). The former might be addressed by advanced EELS simulations, while the latter restricts the number of accessible systems unless suitable external reference states can be identified.

2.2. Study of Space Charge Layers at Heterojunctions by Momentum Resolved Scanning Transmission Electron Microscopy (MRSTEM)

Local potentials at semiconductor junctions are often described in terms of idealized models partially ignoring the true atomic structure of the interfaces affected by, e.g., chemical intermixing, misfit strain, or strain-induced point defects, to name a few. Hence, the development of high-resolution techniques able to spatially map the electric field (or: potential) is of utmost importance. There are two complementary methods to assess local potentials at junctions. The first method is electron holography, which measures the average electric potential projected along the electron beam. Numerous examples of electron holography studies of semiconductor junctions from almost 40 years of research (e.g.,[53–59]) have shown that the technique can successfully be applied to study junctions of various kinds. The second method is momentum resolved STEM (MRSTEM), which measures the gradients of the projected electrostatic potential. These measurements can either be conducted using a pixelated detector or a segmented detector, where the latter method is called differential phase contrast (DPC).[60,61] Here, we want to restrict the discussion to MRSTEM since it can be combined with other analytic techniques (compare S2.2) more easily.

The principle of this method is to scan a focused electron probe across the sample and measure the beam deflection at each scan position. This deflection is proportional to the lateral momentum transferred from sample to electron beam.[62] For sufficiently thin samples, i.e., when the phase object approximation applies, this is proportional to the gradient of the projected electrostatic potential of the sample at the position of the electron probe.[62,63]

In general, all electric potential gradients inside a sample contribute to the acquired MRSTEM signal. Therefore, it is possible to map projected potential gradients of individual atomic columns with this method.[64,65] With regard to photovoltaic applications built-in potentials and band discontinuities at junctions are of higher relevance. The gradients of these potentials, however, are orders of magnitude smaller than those of atomic potentials. In order to still be able to measure nanometer sized potential gradients, one can take advantage of a probe size much larger than the lateral extension of atomic potentials, e.g. ≈1 nm. Nevertheless, the large atomic potentials affect the MRSTEM signal via multiple scattering. In order to mitigate this issue, it is helpful to tilt the sample away from zone axis conditions[66] and to precess the incident electron beam.[67,68] For heterojunctions, the situation is further complicated by an abrupt change of the mean inner potential (MIP) at the interface and changes of the atomic structure across heterointerfaces.

Nonetheless, there are several examples where MRSTEM has been employed successfully to measure potential gradients across interfaces. Beyer et al. showed that doping concentration, polarity, and depletion regions can be measured quantitatively for GaAs p-n junctions,[69] da Silva et al. used in situ biasing of

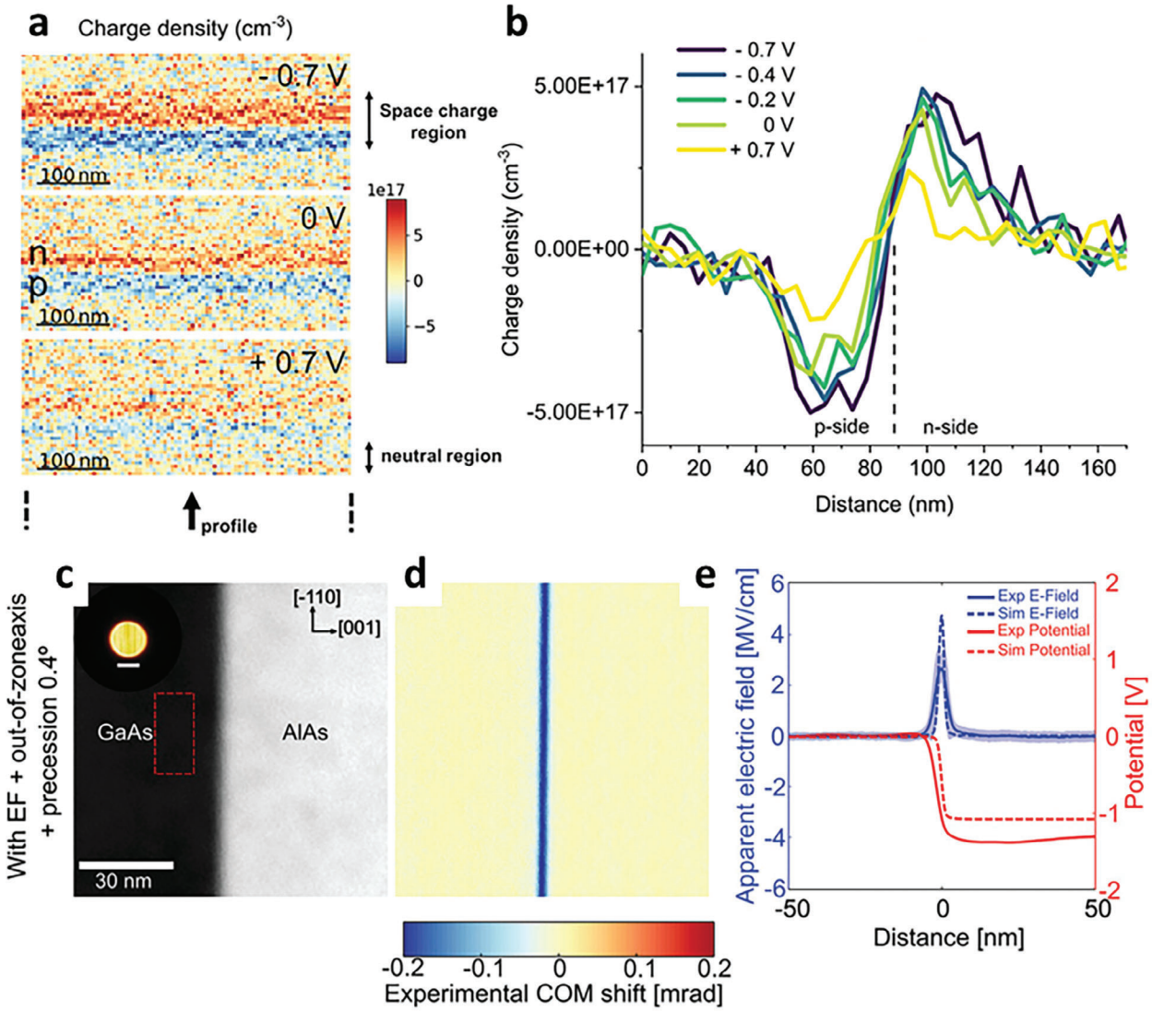

Figure 3. MRSTEM measurements at junctions. The images a) and b) depict the charge density at a Si p-n junction for different biases. Reproduced with permission,[66] © 2022, published by American Chemical Society. The images c) to e) show the electric field and potential across a GaAs/AlAs heterojunction, reproduced under terms of the CC-BY license,[70] © 2023 The Authors. Small Methods published by Wiley-VCH.

symmetrically doped Si p-n junctions in combination with MRSTEM to measure the doping gradient at a junction,[66] **Figure** 3a,b), and Chejarla et al. demonstrated quantitative measurements of nanometer-sized potential gradients across a GaAs/AlAs heterointerface with MRSTEM,[70] Figure 3c–e). Combining in situ biasing MRSTEM measurements with accurate MIP values would enable to separate built-in potentials from MIPs and to measure the exact band bending for heterojunctions.

2.3. Excess Charge Carrier Separation and Recombination Studied by Scanning Transmission Electron-beam-Induced Current (STEM-EBIC)

To characterize the response of charge-separating devices to local excitations of electrons and holes, electron be am induced current (EBIC) measurements can be performed by scanning a focused electron probe across the device and collecting the resulting short-circuit current. This approach has been used in the scanning electron microscopy community for several decades[71–74] and – leveraged by the development of modern biasing TEM holders and reliable sample preparation methods – has been transferred to the TEM recently.[75–78] Importantly, the current signal caused by the electron beam interaction can include several components such as the current due to separation of excess electrons and holes in a charge-separating device or due to refilling of holes caused by secondary electron emission. The latter is also referred to as STEM-SEEBIC and can for example be utilized to study the local conductivity,[79] the morphology of nanoparticles,[80] or the secondary electron yield on the atomic scale.[12,81] However, since this section focuses on the characterization of solar cells, the emphasis is put on the former case which

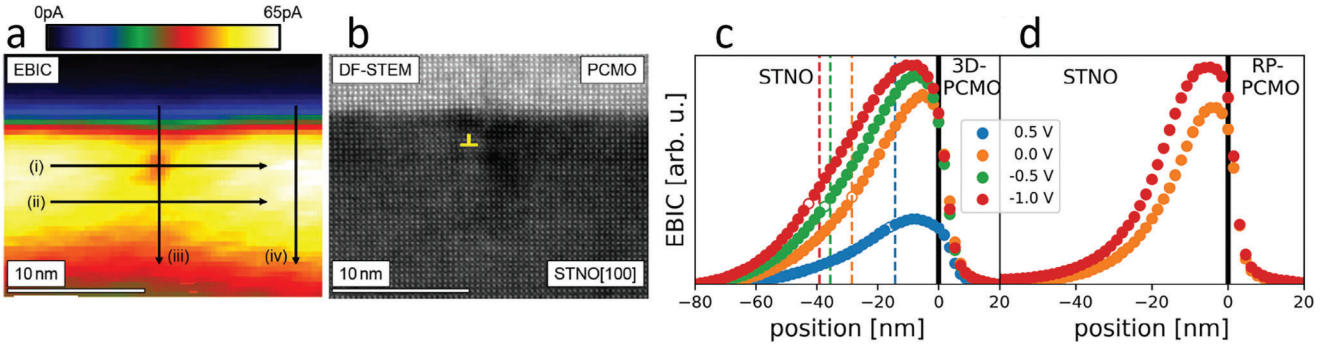

Figure 4. Examples of STEM-EBIC at p-n heterojunctions. Top row: STEM-EBIC map (left) and simultaneously recorded STEM darkfield image (right) of a misfit dislocation in STNO taken at the p-n heterojunction between STNO and PCMO. Adapted under the terms of the CC-BY license.[77] © 2019, The Authors, published by IOP Publishing. The STEM-EBIC map shows a strongly reduced signal due to excess carrier recombination at the dislocation core. Bottom row: STEM-EBIC profiles at different bias voltages obtained for an STNO/PCMO a) and an STNO/RP-PCMO junction b). The extension of the profile reflects the space charge region width (see dashed lines in a)), their amplitude the charge collection efficiency of the junction, which is strongly reduced at zero bias. Reproduced under terms of the CC-BY license,[45] © 2023, The Author, published by eDiss-SUB Göttingen.

is referred to as STEM-EBIC and typically yields current signals around two orders of magnitude higher than STEM-SEEBIC.

The primary goal of STEM-EBIC is to enable a high spatial resolution allowing the investigation of materials with diffusion and screening lengths, space charge layer extensions as well as the impact of extended defects on excess carrier recombination on the nanometer range, which is severely limited due to the extended interaction volume of the electron beam with the specimen resulting from to multiple scattering in SEM-EBIC.[43] In fact, due to the high kinetic energy of the primary electrons and the low sample thickness in the TEM, the resulting beam spread is in many cases negligible and for example, enhanced recombination in the vicinity of misfit dislocations can be observed with nanometer resolution.[77] **Figure 4** (top row) shows the example of a misfit dislocation in Nb-doped $SrTiO_3$ (STNO) close to the interface to a (p-doped) $Pr_{0.67}Ca_{0.33}MnO_3$ (PCMO) layer.

A major challenge is the thin foil extraction during TEM sample preparation since (i) electrical connections need to be established while undesired short circuits need to be avoided.[82] Furthermore, (ii) it results in poorly defined and typically highly damaged surfaces causing strong recombination of excess charge carriers and potentially additional space charge layers absent in the bulk. A major achievement in the field of STEM-EBIC was the introduction of a model accounting for both bulk and surface recombination in terms of an effective diffusion length and thus disentangling the two effects enabling the quantification of nanometer bulk diffusion lengths.[83] We note here, that on the basis of this model, STEBIC maps can be simulated quantitatively by two-dimensional finite-element calculations.[84] So far, this model is limited to neutral materials, however, if an extension of the model including electric field effects is found, STEM-EBIC could serve as a method to extract minority carrier diffusion lengths and electric field strengths simultaneously in the future.

2.4. Controlling Telegraph Noise in a Few-donors System by Laser Illumination

The influence of interfaces, surfaces, and defects at the atomic level is becoming increasingly important in the miniaturization of solid-state systems. Semiconductor devices are prototypically systems that have been thoroughly investigated in the past. Besides technological challenges in the ongoing miniaturization process of cutting-edge semiconductor devices, the understanding and controlling of charge dynamics on the atomic scale requires new experimental approaches.

Dopant atoms are essential for the operation of semiconductor devices because of the free charge carriers they add to the material. With the downscaling of these structures, properties of individual dopant atoms start to play a role in their functionality. The influence of a single dopant atom on its surrounding environment can be studied with scanning tunneling microscopy (STM).

Scanning tunneling microscopy and spectroscopy have given access to the structure and properties of individual and few-atom doping systems.[13,14,85,86] Moreover, combining STM/STS with optical excitation (**Figure 5**, top panel a) has opened a new path to the dynamical properties of such systems. Many technical challenges for pulsed excitation within an STM setup have been solved in the last decade.[87–89] We use pulsed optical excitation in combination with scanning tunneling microscopy at the n-doped GaAs (110) surface to investigate single donor dynamics within a nanoscale, localized space charge region (Figure 5 top panel b). The tip of a scanning tunneling microscope is on the one hand used to prepare a nanoscale space charge region including the injection of electrons and at the same time allows to analyze the resulting time evolution of the excited system. More specifically, our approach gives access to the dynamics of the transition between the charged and the neutral state of single and few dopant atom systems, as a protype Si in GaAs was chosen. In a first approach, we studied the charging processes of individual doping atoms including the interaction of those atoms with their surroundings.[90,91] In addition, tuning the tunneling rate can drive the system into nonequilibrium conditions. This allows us to distinguish between the decay of optically induced free charge carriers and the decay of donor charge states. The latter process is atomically resolved and discussed with respect to donor-level binding energies and local donor configurations.[91] It gives access to the decay of optically induced free charge carriers and the decay of donor charge states. While optical spectroscopy from the

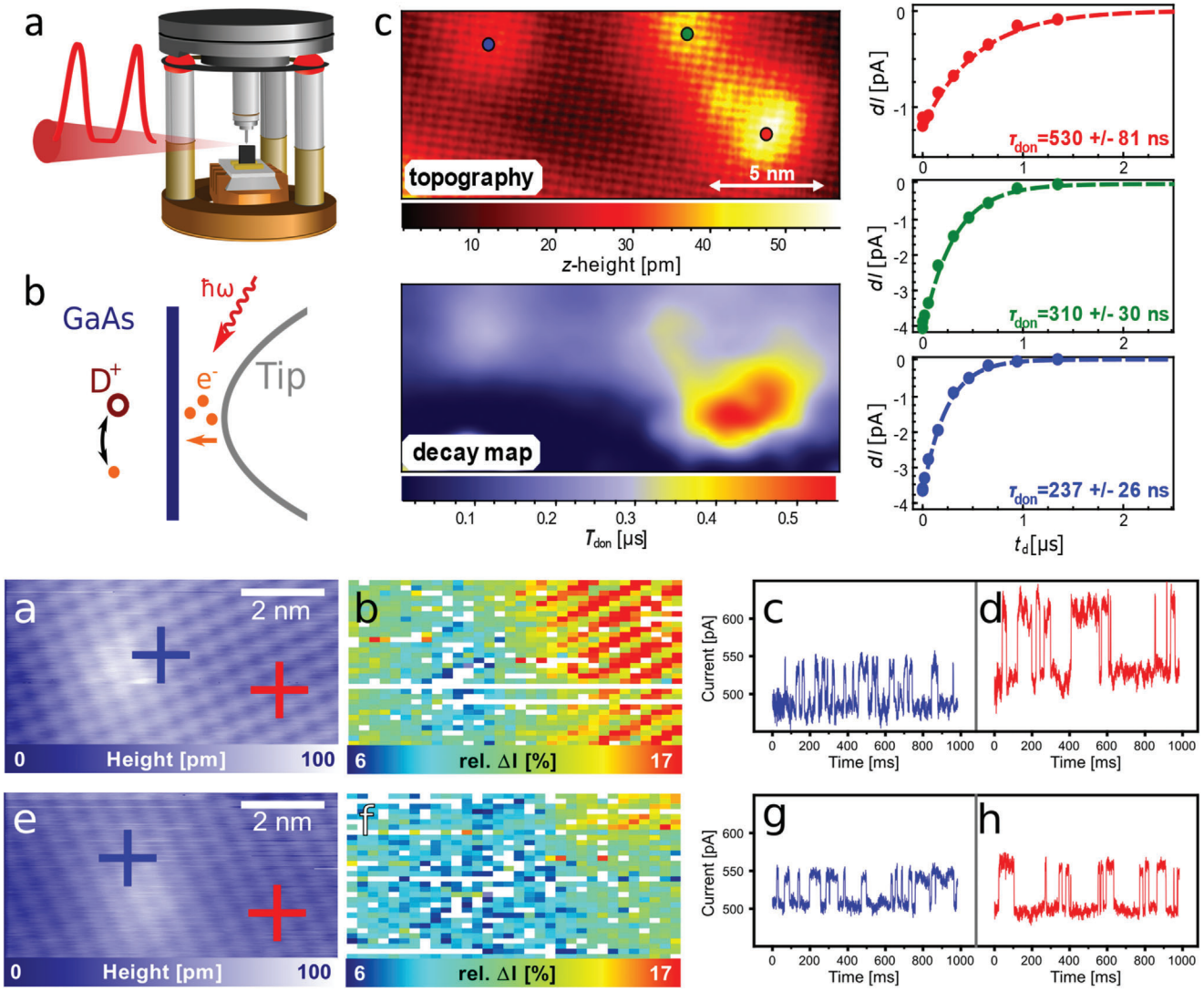

Figure 5. Top panel: a) Combining STM with optical excitation allows to investigate the dynamics of few-donor systems. b) Applying a voltage between the STM-tip and the GaAs (110) surface, the charge state of donors can be tuned. The tunnel current as well as optical excitation can modify the charge state. c) Atomically resolved (Topography) decay maps of the excited system show a strong spatial variation. The right colomn shows three individual decay curves, the color corresponds to the position marked within the topography. (Reproduced with permission from,[91] ©2017, published by 'The American Association for the Advancement of Science'). Bottom panel: Data comparing the fluctuation between dark conditions and illuminated conditions. A) Topography of GaAs under dark conditions. c,d) Time series of the tunneling current recorded for fixed tip-sample distance at the positions indicated by the colored dots in a). b) Spatial map of the relative telegraph step height; e) topography of GaAs under illumination. g,h) Time series of the tunneling current recorded for fixed tip-sample distance at the positions indicated by the colored dots in e. f Spatial map of the relative telegraph step height.

1980s has characterized the relaxation of Si donors with single time constant, locally resolved spectroscopy has shown that the relaxation time depends strongly on the distance of the donor to the surface and shows a spread up to a factor of 5 (Figure 5 top panel c).[91]

While such nanosecond dynamics is expected for an atomic scale system, STM has also shown blinking on much longer time scales.[85] It has been shown that laser excitation of GaAs can be used to control the noise characteristic of the tunneling current on GaAs(110).[14] Well-known mechanisms causing noise are the discrete charging and discharging of donors resulting in discrete jumps in the tunnel current, the same process discussed above. We investigate the influence of light-induced charge carriers on telegraphic fluctuations[92] of the tunnel current caused by erratic switching of the charging state of donors.

For fixed tip-sample distance, the resulting charge fluctuations cause a random switching of the tunneling current between two well-defined levels, observable as a telegraph signal (Figure 5 bottom panel c,d,g,h). Comparison of tunnel current time series recorded at different lateral tip positions gives access to spatial variations of the signal with atomic-scale precision. Optically excitation of the system with an energy larger than the bandgap induces minority charge carriers into the space charge region. The concentration of free charge carriers accumulating below the tip is controlled by the tunnel current. This allows to investigate the effect of a low-density hole gas on the non-equilibrium donor

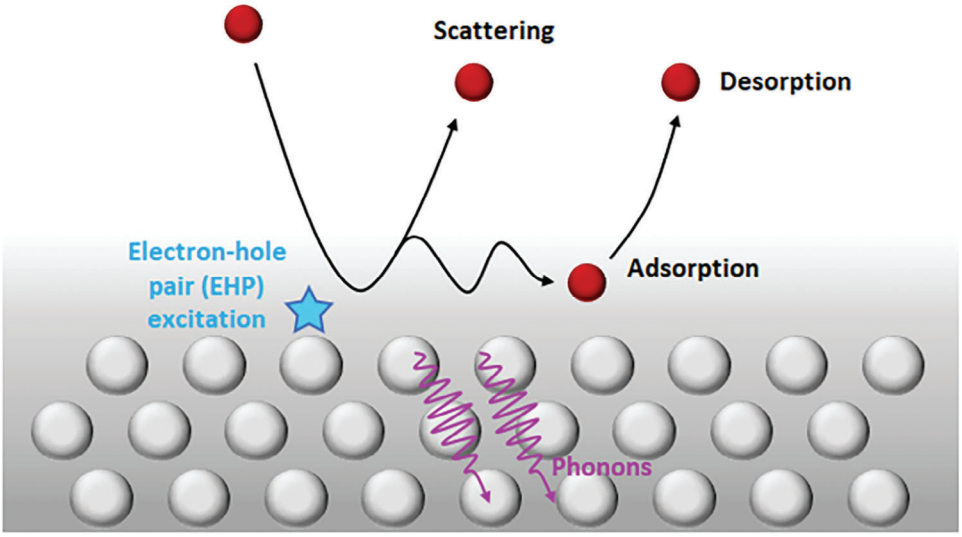

Figure 6. Energy dissipation at surfaces. When an atom or molecule approaches a surface, it can exchange its energy with the different degrees of freedom of the solid. The efficiency of these atomic-scale processes determines whether the molecule scatters back or is adsorbed to the surface. It also determines how much of the kinetic energy at a sliding contact is lost as friction, by exciting degrees of freedom in the solid.

charging events. The optical excitation is found to reduce the telegraphic step height as well as to increase in the switching rate. We interpret this change of the noise in the few-donors system as a lowering of the energy barrier between the metastable states in the non-equilibrium configuration.

The telegraph noise is attributed to one-electron charging processes. The light-induced charges are mobile, homogenizing the surface potential landscape. The charges reduce the potential variation at the tunneling junction, thereby decreasing the telegraphic step height. In presence of the hole gas the tunneling probability into the donor state is increased leading to reduced lifetimes of both charge states.

3. Atomic-Scale Mechanisms for Dissipation at Surfaces

To control surface processes like catalysis, electrochemistry, and photoactivated reactions, which are of fundamental importance, we must understand the mechanisms and dynamics of energy dissipation and how surface and sub-surface properties influence these processes (see Error! Reference source not found.). Dissipation at surfaces determines the rates and efficiencies of the energy conversion processes occurring there. For example, the formation of chemical bonds of a molecule on a surface requires the dissipation of its kinetic energy.[93] Even the motion of physisorbed molecules on a surface, such as occurs when two contacting surfaces slide by each other, leads to irreversible energy loss. Nonetheless, our understanding of surface dissipation is quite limited and requires clarification of atomic-scale and quantum mechanisms. Advances in experimental highly sensitive surface methods based on sliding tips and inelastic scattering of atoms or molecules combined with simulation methods are opening access to these mechanisms of dissipation, but their connection to macroscopic parameters and empirical laws is still wide open.[94–96] For example, we do not yet know what atomic scale processes determine the friction coefficient or which degrees of freedom determine damping or internal friction.[94]

In this chapter, we present two methods that provide deep insights into atomic-scale mechanisms of energy dissipation. First, we describe AFM-based methods that reveal the role of sub-surface properties in the dissipation of mechanical and kinetic energy deposited at the surface. Second, we examine the dynamics of bond formation and breaking at surfaces by inelastic H-atom scattering using Rydberg atom tagging to gain a deeper understanding of how energy transfer mechanisms between molecules in the gas phase and surfaces are affected by surface properties. Ultimately, these methods aim to identify the contributions of electrons, phonons, spins, and their interactions to energy dissipation (Figure 6).

3.1. Control of Friction Through Material Properties

Friction describes the loss of kinetic and mechanical energy that occurs when two surfaces approach or slide by each other.[94,97] The friction or dissipated energy is known to depend sensitively on exact surface chemistry and morphology, but a number of recent AFM-based studies have also revealed that the sub-surface material properties play a decisive role.[98–103] Specifically, it has been found that the measured nanoscale friction seems to correlate with electronic degrees of freedom, although the friction changes are much larger than predicted by theoretical considerations. In addition, one recent study reveals significant contributions to nanoscale friction from the phonon degrees of freedom.[103] The importance of material properties in determining friction not only raises fascinating insights into the routes for energy dissipation, it also offers a potentially practical approach to controlling friction. While surface chemistry and morphology are difficult to control during use, the material properties can be controlled by material selection and even actively controlled by

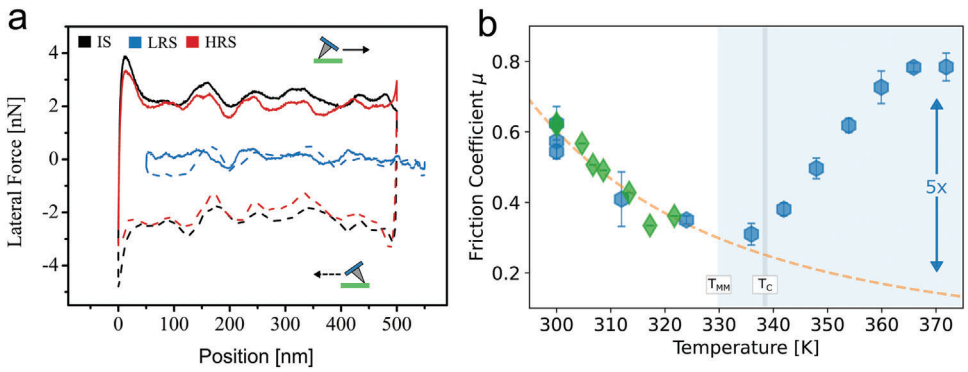

Figure 7. Reversible control of friction at a manganite surface. AFM-based lateral force microscopy is used to measure the friction during phase transformations in manganite films. a) Lateral force friction loops for a $La_{0.55}Ca_{0.45}MnO_3$ film in the initial insulating state (IS = black), after resistively switching to the conducting state (LRS = blue), and after resistively switching back to the insulating state (HRS = red). Resistive switching was achieved by applying an electrical potential between the Pt-coated Si AFM tip and the film surface. The friction is proportional to the area between the forward (solid line) and backward (dashed line) lateral force traces and is larger in the insulating state than in the conducting state. (Reproduced with permission,[104] 2020, ©American Physical Society) b) Reversible changes in the friction coefficient are shown during heating and cooling between the low-temperature ferromagnetic state and the high-temperature paramagnetic polaronic conductor state of a $La_{0.7}Sr_{0.3}MnO_3$ film. Friction in the low-temperature phase is controlled by thermolubricity (the dashed line fit shows the expected Arrhenius dependence), while the high-temperature phase exhibits a factor five increase in friction due to dissipation by polarons.[105] (Adapted from,[105] 2021, John Wiley-VCH).

transformations induced by external fields such as temperature or electric potential.

At the macroscopic level, friction between two sliding bodies is well described by phenomenological equations that consider dissipation in the true contact area due to plastic events that generate heat, defects, and structural changes. However, little was known about the underlying mechanisms for these plastic events until the development of atomic force microscopy (AFM) methods in the 1980s. This opened up the possibility to measure dissipation between an AFM tip and a surface in a controlled way at the nanometer scale and to correlate the losses with local properties. The most common method to quantify friction involves measuring the force needed to slide an AFM tip along a surface (lateral force microscopy); much smaller contributions from dissipative losses between surfaces in near contact can also be accessed using so-called dynamic AFM methods. The information about local friction can then be directly compared to AFM-based measurements of local properties, such as conductivity, charge states, work functions, elastic and plastic behavior. Thus AFM-based studies now provide quantitative information about energy losses in nanometer size contact interfaces, which can be correlated with local atomic and quantum properties.

Our AFM-based friction studies have focused on manganite films as a model material system because (i) their properties can be sensitively controlled through stoichiometry and structure, and (ii) manganites exhibit strong coupling between degrees of freedom, in particular between electrons and phonons, leading to subtle effects and diverse tactics for control. Two examples of the dependence of friction on manganite film properties are shown in **Figure 7**. In the first example, we find that friction can be reversibly switched between high and low values by resistively switching the film between high and low resistive states.[104] We argue that the friction is limited by phonon relaxation times, which are strongly coupled to the electronic degrees of freedom through distortions of the MnO_6 octahedra. The high resistive state is believed to be a polaronic conducting state involving strong coupling between phonons and electrons. The low resistive state is metallic and the friction is lower because the mechanical distortions introduced by the sliding tip do not couple so strongly to the electronic degrees of freedom. In the second example, friction is observed to increase steeply as a film is heated through the transformation temperature from a low-resistance ferromagnetic state to a high-resistance paramagnetic state.[105] The excess friction is also attributed here to the presence of polarons, which are presumably stimulated by the stick-slip excitations generated at the sliding contact. These two examples reveal the importance of coupled atomic-quantum excitations in dissipation and illustrate the possibility to tune friction through atomic and quantum materials properties. Materials with variable electron-phonon or spin-phonon couplings are promising candidates for controlling friction.

A more recent study of friction at the surface of superlattice manganite films shows even more clearly that friction depends on sub-surface material properties. AFM measurements confirm that nanoscale friction at a surface can be controlled by varying how deep a layer of different material is buried below the surface,[106] as has been predicted by models based on viscous losses.[107] This opens the possibility to locally tailor friction at a surface without changing the surface materials, by varying the surface layer thicknesses and optimizing the materials below.

3.2. Understanding the Dynamics of Bond Formation and Breaking at Surfaces by Using Rydberg Atom Tagging

When an atom or molecule hits a surface, the ability to efficiently transfer its kinetic energy to the surface determines whether it will be adsorbed or scattered. Inelastic scattering experiments allow to study the energy transfer between an atom or molecule and a surface, revealing the important pathways for energy dissipation that facilitate adsorption. In most inelastic surface scattering experiments molecules are used. Early experiments focused

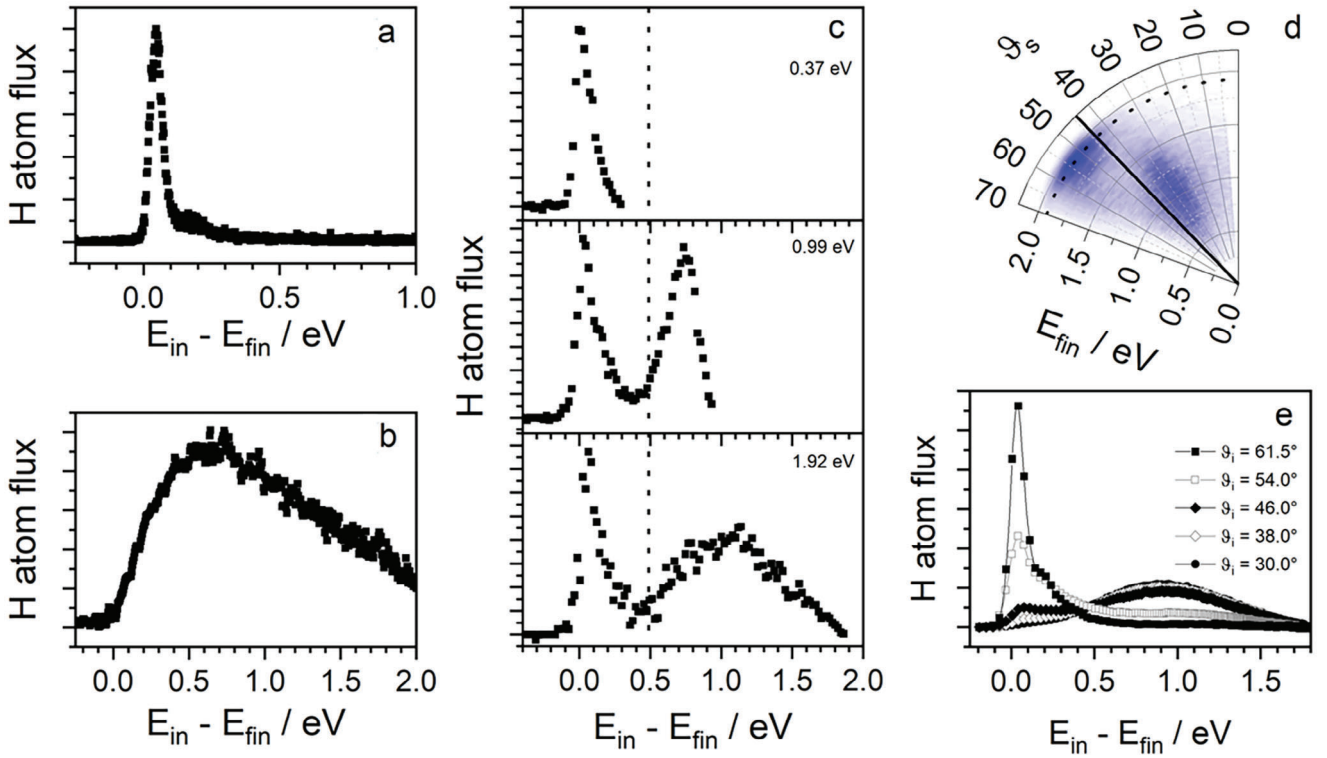

Figure 8. Energy loss of H atoms scattered from various surfaces. a) Insulator surface: solid Xe, incidence energy $E_{in} = 2.76$ eV, incidence angle $\vartheta_{in} = 45°$, scattering angle $\vartheta_s = 45°$, and surface temperature $T_{sur} = 45$ K.[113] b) Metal surface: Au(111), $E_{in} = 2.76$ eV, $\vartheta_{in} = 45°$, $\vartheta_s = 45°$, $T_{sur} = 300$ K.[114] c) Semiconductor surface: Ge(111)c(2 × 8) for three different incidence energies, $\vartheta_{in} = 45°$, $\vartheta_s = 45°$, $T_{sur} = 300$ K.[115] (d+e): Graphene on Pt(111): d) Angular resolved kinetic energy distribution for an incident angle of 44° (solid black line marks specular angel, dotted line marks incidence energy of 1.92 eV). e) Scattering angle integrated energy loss distributions for an incidence energy of 1.92 eV and various incidence angles.[116]

on the rotational excitations of the scattered molecules.[108] Later, the coupling of the molecular vibrations to surface excitations became of central interest.[93] Today, experiments have improved to the point that all degrees of freedom can be controlled and determined simultaneously.[95] Using rare-gas atoms, information about surface phonons[109] and adsorption mechanisms can be obtained.[110] However, they tell us little about surface chemistry. The H-atom, being a radical, can form a short-lived transient bond with the surface during the scattering process. This transient bond formation can open very efficient energy transfer pathways into the phonon and electronic modes of the surface.[96]

Over the last decade, we have developed a new instrument to study the inelastic scattering of individual H-atoms from surfaces. The instrument combines the techniques of photolysis of hydrogen halide molecules to form a mono-energetic H-atom beam and Rydberg-Atom-Tagging for the detection of the scattered H-atoms[17,111] with an ultra-high vacuum surface scattering apparatus. A detailed description of the H-atom scattering apparatus can be found in Ref. [96,112] In short, a nearly mono-energetic hydrogen atom beam is generated by the photolysis of hydrogen halide molecules. Variation of the photolysis laser wavelength allows the generation of H-atom beams with kinetic energies in the range of a few 100 meV up to 7 eV. The beam is pointed onto the sample surface and the angular and kinetic energy distribution of the scattered H atoms is analyzed using Rydberg atom tagging.[111] Thereby, the H atoms are excited to a high Rydberg state and fly a known distance before they are field-ionized and detected. Rydberg tagging provides a high-resolution, highly sensitive, and nearly background-free probe that was essential for the experiments. The detector is rotatable, enabling time-of-flight distribution measurements at a variety of scattering angles.

This new instrument allows high-resolution studies of the energy loss of hydrogen atoms scattered from surfaces. The obtained angular and energy distributions give detailed information about the energy dissipation pathways. They provide a benchmark for the construction of potential energy surfaces and for simulations of the underlying dynamics.

Figure 8 shows the results for 4 different materials: an insulator, a metal, a semiconductor, and the 2D material graphene. In case of the very simple insulator of solid Xe, the energy transfer is limited to phonons excitation and since the mass mismatch between H and Xe is large, the energy transfer is marginal (Figure 8a).[113] For a metal surface like Au(111), way more energy is transferred in the scattering event (Figure 8b). The underlying reason is an efficient transfer of the kinetic energy of the impinging H-atoms to electronic excitations of the surface that is not possible in an insulator.[114] For a semiconducting surface like Ge(111)c(2 × 8) the energy transfer is limited to phonons for incidence energies below the surface band gap (top panel Figure 8c). For incidence energies above the surface band gap, excitation of electrons over the surface band gap is observed with

high probability.[115] A site-specific process involving a transient bond formation with a particular type of surface atom is proposed as the underlying mechanism.[117] Figure 8d–e shows results for H atom scattering from graphene grown on Pt(111). C—H bond formation on graphene is an activated process and has a barrier. Impinging H atoms can either be scattered from the barrier or pass the barrier to form a C—H bond. The newly formed bond is either stabilized by rapid energy dissipation into the graphene or it breaks again and the H atom is ejected back into vacuum. This leads to a bimodal energy loss distribution, as apparent in the angular resolved energy distribution shown in Figure 8d. The probability for the H atom to cross the barrier scales with normal energy, as shown in Figure 8e. The experiments in combination with molecular dynamics simulations revealed a very efficient energy dissipation pathway into the in-plane phonon modes of the graphene sheet that is facilitated by the transient bond formation.[116]

4. Nanoscale Studies of Phase Transitions to Tune Energy Materials

Phase transitions can happen within a small range of a control parameter and can lead to tremendous changes of material properties that govern excitations and conversion.[118] Their appearance and impact on energy materials need to be considered. In addition, they provide alternative strategies to functionalize energy materials.[42] Prominent examples are phase change materials[119] or the metal-to-insulator transition,[120] either steered by temperature, external parameters like electric or magnetic fields or even induced by optical excitations that are involved in the energy conversion process.[121] The underlying basic principles of phase transitions are often well understood on a macroscopic scale and can be described within a variety of different frameworks.[122] Local effects at surfaces and interfaces, however, remain elusive despite their relevance for energy materials and their potential to be a source of functionality themselves. Simple bulk thermodynamic principles based on the nature of order parameters allow to classify the transition with respect to the degree of order but need to be extended to spatially inhomogeneous phenomena involving nm length scales, where local in situ diffraction methods based on small electron probes in transmission electron microscopy (TEM) as well as ultrafast TEM (UTEM) are providing valuable insight into the spatial characteristics or spatio-temporal evolution of order parameter. Bulk phases can be modified at surfaces and interfaces, for example, due to lattice strain,[123] point defects,[124] or other types of chemical inhomogeneities. 2D materials and atomic layers on surfaces allow for phase tuning by various optical, geometrical, and chemical processes, including a modification of thermal phase transitions[125] that, e.g., can have a huge impact on dissipative processes.[126]

Furthermore, an intense laser pulse in a UTEM can provoke light-induced phase transformations, which can subsequently be observed using an electron pulse, realizing a pump-probe scheme.[127] Here, spatio-temporal dynamics of energy materials can be visualized on a fs-ns time and nm length scale. As both the stimuli to steer the phase transition as well as the involved timescales strongly differ in TEM and UTEM experiments, they are described in two separate sections, i.e., Section 4.1 and 4.4. In addition to local electron probes, the progress of surface-sensitive

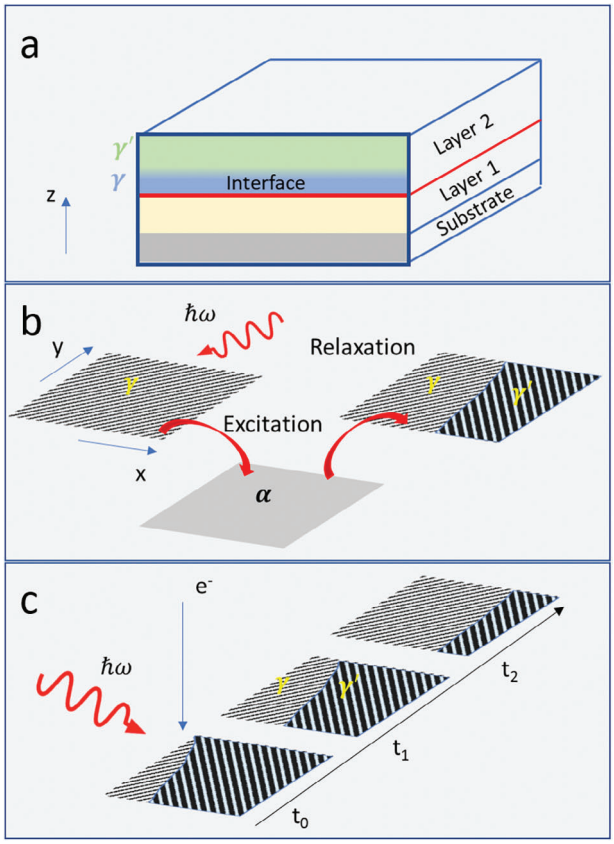

Figure 9. a) Local alteration of bulk phase transitions at interfaces and surfaces. b) Study of local optical excitations at a domain structure by scanning near-field optical microscopy and scanning tunneling microscopy. Spatio-temporal studies of optical-induced phase transition from the γ- to the γ'-phase with inhomogeneous relaxation and c) movement of domain boundaries.

techniques such as low-energy electron diffraction and scanning tunneling microscopy (STM) allow access to ordering phenomena, domain patterns as well as related local electron states. In particular, in low- or 2D systems pronounced collective effects are observed,[21] such as charge density wave formation induced by a Peierls instability, metal-insulator transitions, non-Fermi liquid behavior, or soliton excitations.[128] Here, scanning probe methods like scanning near field optical microscopy (SNOM) and (STM) allow to correlate local electronic and structural degrees of freedom.

Figure 9 schematically shows some of the main application fields of these space- and time-resolved techniques. Specific examples, demonstrating the huge progress in imaging of local phase evolution and its impact on excitations and conversion are shown in the following subsections.

4.1. Phase Transitions in Perovskite Oxides Studied by In Situ TEM

In situ transmission electron microscopy has been developed to a level, where studies of phase transformations induced by varying the temperature, mechanical force fields, and external electric or

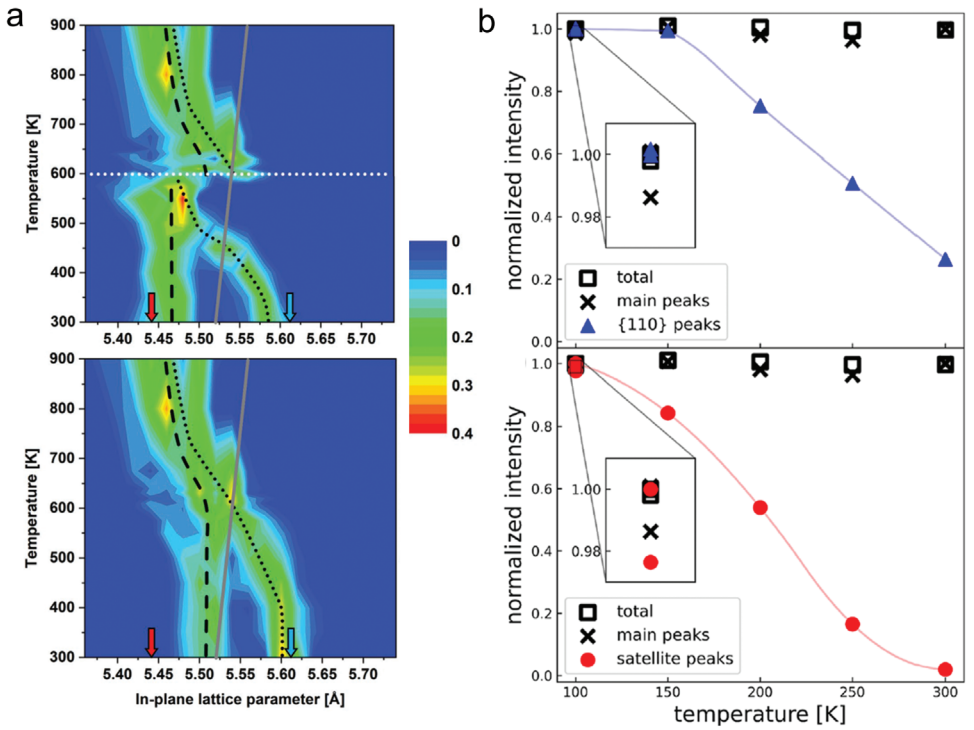

Figure 10. a) Orthorhombic to tetragonal structural phase transition in a $Pr_{0.9}Ca_{0.1}MnO_3$ thin film revealed by in situ heating and environmental 4D-STEM. Adapted with permission from,[137] ©2021, Wiley-VCH. b) Orthorhombic to less orthorhombic structural phase transition (upper plot) as well as charge and orbital order transition (lower plot) in a $Pr_{0.55}Ca_{1.45}MnO_4$ thin film observed by in situ cooling and SAED (reproduced under the terms of CC BY 4.0, ©2024, The Authors, published by AIP Publishing LLC).

magnetic fields on a nm scale have become possible.[11,129] Main challenge is to find contrast mechanisms suitable to observe the corresponding order parameters. Furthermore, observed phase transformations can be altered due to sample preparation, since TEM specimens need to be electron-transparent and thus are typically of a thickness of a few hundred nanometers.

Recent developments of in situ TEM methods using different sample stimuli have been reviewed by Han et al.[11] demonstrating electrical biasing, heating, cooling, magnetizing, light illumination, and mechanical testing. Furthermore, the chemical environment can be controlled to some extent by employing closed-cell gas or liquid holders[130,131] or an open-cell environmental TEM (ETEM).[30]

At the same time, the set of observables – and thus possible order parameters for phase transitions – that can be measured with high precision in the TEM has been constantly expanded and includes for example electric potentials or fields,[62] polarizations,[132] magnetizations,[133] or strain fields.[134] Particularly the development of four-dimensional scanning TEM (4D-STEM) in conjunction with modern electron detectors enables a flexible trade-off between spatial resolution and sensitivity for most of the mentioned observables depending on the needs of the experiment.[135] Furthermore, electron energy loss spectroscopy (EELS) can be used to measure for example chemical compositions, valence states, or band gaps.[136]

Two specific examples of phase transitions related to energy conversion are presented in **Figure 10a**. The orthorhombic to tetragonal structural phase transition in a $Pr_{0.9}Ca_{0.1}MnO_3$ thin film was proven by Meyer et al.[137] utilizing in situ heating in conjunction with 4D-STEM to locally extract the lattice constants in a nanodomain structure. An additional control of the oxygen partial pressure in an ETEM was needed to avoid irreversible oxygen loss occurring under ultra-high vacuum conditions. Figure 10b. Both an orthorhombic to less orthorhombic structural as well as a charge and orbital order phase transition in a $Pr_{0.55}Ca_{1.45}MnO_4$ thin film was found by Flathmann et al.[138] combining in situ cooling and selected area electron diffraction (SAED). In addition to the proof of occurrence of the structural phase transitions in the presence of epitaxial strain and related defects, changes in critical temperatures and local order parameter fluctuations in the vicinity of defects were demonstrated. In conjunction with the TEM studies, photovoltaic measurements were conducted on the same thin films and it was shown that the onset of the photovoltaic effect correlates with the orbital order phase transition in $Pr_{0.9}Ca_{0.1}MnO_3$[139] and the charge and orbital ordered phase in $Pr_{0.55}Ca_{1.45}MnO_4$.[42] Separating phase transitions in the octahedral tilt system from orbital and charge ordering led to the conclusion that hot polaron stabilization required for the photovoltaic effect is caused by the electronic order.[139]

4.2. Local Studies of Phase Transitions in van-der-Waals Materials by Using Scanning Near Field Optical Microscopy (SNOM)

Materials that show a change of optical properties in phase transitions are not only promising for control of light-harvesting

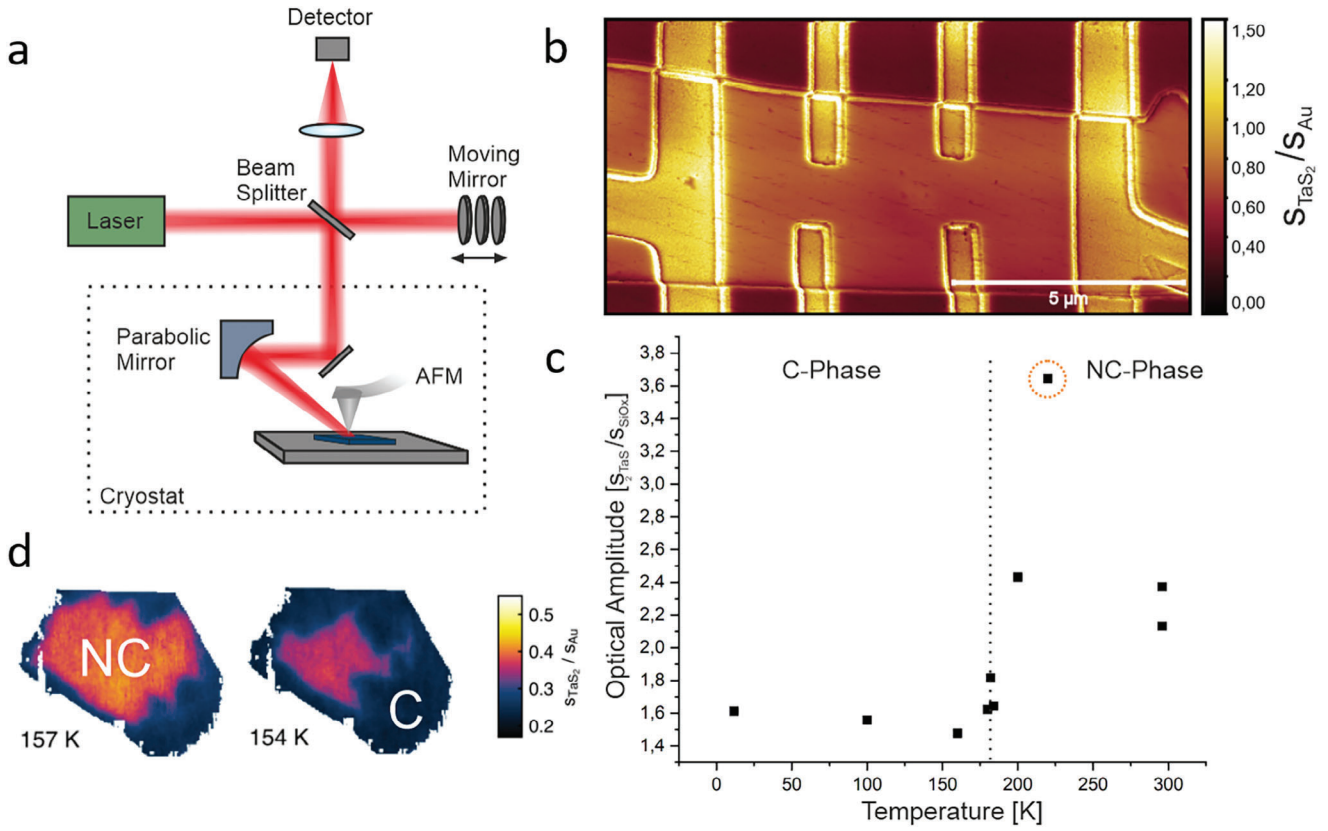

Figure 11. a) Schematic SNOM setup with an interferometer and an oscillating mirror. Sample can be placed in a cryostat to measure temperature-dependent optical response. b) Typical amplitude SNOM image of a TaS_2 flake normalized to gold at 12K at a wavelength of 10,675 µm. c) Contrast of TaS_2 to SiO_x at different temperatures. Jump in contrast at ≈180K corresponds to the phase transition between C-NC. Outlier at 220K is due to bad image quality. d) Real-space imaging of NC-C phase transition upon cooling. Reprinted figure with permission from,[146] Copyright 2018 by the American Physical Society.

but also for future energy-efficient device applications.[140,141] Particularly interesting are novel 2D materials that exhibit stable states and/or fast transition times such as the prototypical charge density wave material TaS_2.[21] Here, properties such thermoelectric[142] and optical response[143] drastically change at the phase transition between different charge density wave (CDW) states. Remarkably, electron (n-type) conductivity in the nearly commensurate (NC) phase turns into hole (p-type) conductivity in the commensurate (C) state.[144] An understanding of such materials requires local optical probes, as, e.g., scanning near field optical microscopy (SNOM). It allows to laterally resolve with a few tens of nanometer lateral resolution the optical properties of materials.[145]

A typical SNOM setup is schematically shown in **Figure 11a**. A (usually monochromatic) laser source is focused on an oscillating AFM tip, which resides close to the surface. The tip creates a near-field below the tip apex which is strongly correlated to the oscillation frequency of the tip. Detecting the backscattered light at higher harmonics of the tip frequency allows to reduce the effect of the far-field contribution as this is not influenced by the tip oscillation. The backscattered light is collected with the use of an interferometer and an oscillating mirror in the delay line. Thus, the phase and amplitude of the signal can be decoupled.[145] As the intensity and phase of the backscattered light depend on the material properties, its optical conductivity can be resolved with nanoscale resolution and far below the diffraction limit, which is the limiting factor in most laser measurement techniques. SNOM is, therefore, a suitable technique to resolve changes in the current phase state, to track the spatio-temporal variation of states upon changes of external fields, and to measure the resulting local variation of excitations in the visible and IR range.[146]

Figure 11b,c shows the local optical response of the transition metal dichalcogenide 1T-TaS_2 as a van-der-Waals material with controllable conductivity. It shows phase transitions between different charge density wave ordering, such as commensurate to non-commensurate, which are not fully understood.[147] A typical SNOM amplitude image of a contacted TaS_2 is shown in Figure 11b.

Since phase transitions occur at temperatures below 300K, a special type of SNOM is required for the investigations that allow imaging down to cryogenic temperatures. Figure 11c shows the temperature dependence of the optical amplitude contrast between TaS_2 and SiO_x. The phase transition between the insulating commensurate (C)-Phase (<180K) and the more conductive nearly-commensurate (NC) state (>180K) results in a sudden jump in optical contrast from ≈1.6 to ≈2.4. at ≈180 K and can be also monitored by electrical transport measurement.[147] As shown by Frenzel et al.[146] this phase transition can also be

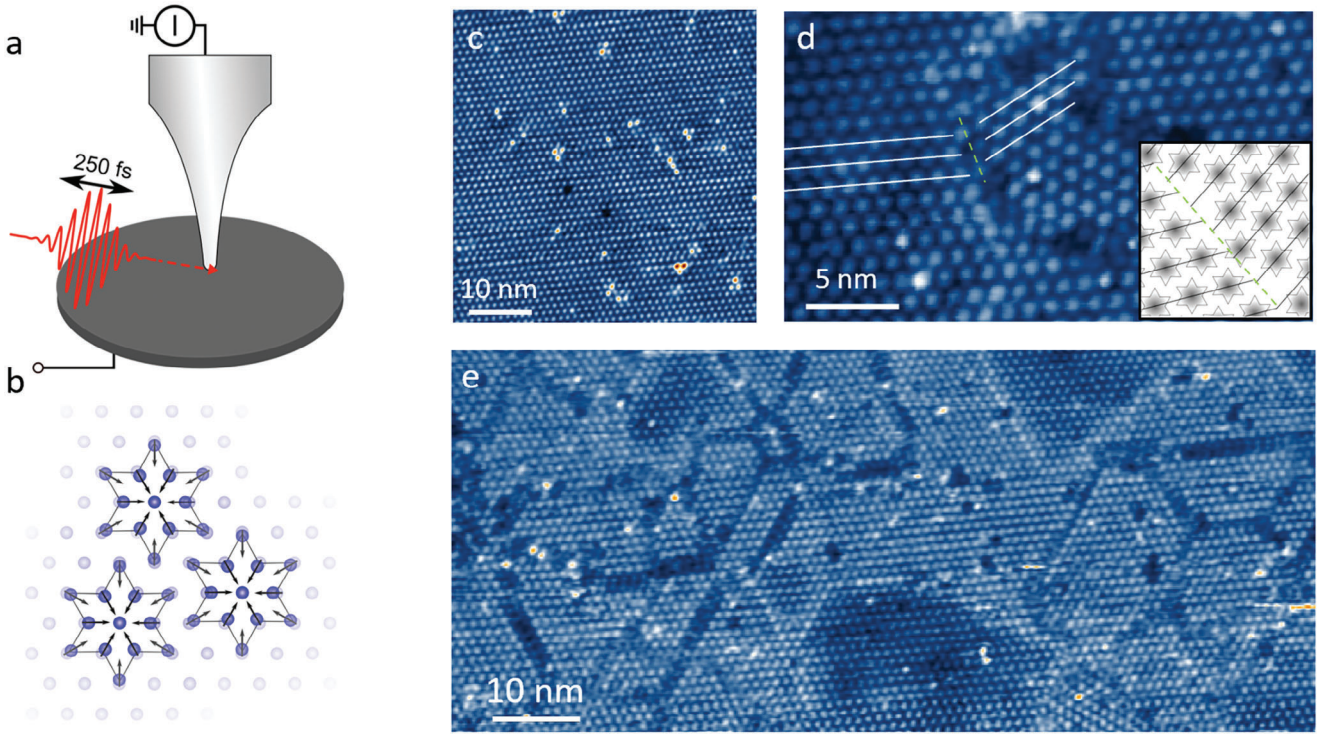

Figure 12. A sketch of a scanning tunneling microscope tip in combination with pulsed optical excitation and an illustration the star-like groups of Ta-atoms forming the $\sqrt{13}\times\sqrt{13}$ R13.9°-reconstruction are shown in a) and b), respectively. The resulting CDW can be resolved by STM constant-current topographies c–e). A formerly homogeneously reconstructed surface before c) and after intense laser excitation d,e). The rotational degree of freedom resulted in a chiral domain boundary, which is indicated by the white lines and illustrated in the inset. e) Zoom-out of the same area as in c showing a variety of phases and defects.

followed in real space so that domain growth as a function of temperature can be monitored with nanoscale spatial resolution (Figure 11d).

In contrast to the observation of a domain-like growth of the NC-CDW phase out of the C-phase upon heating reported by Frenzel et al.[146] we see a homogeneous phase change which is attributed to different defect densities of the samples. Combining electrical switching[148,149] with SNOM imaging or using additional laser sources for switching[150] can unlock additional metastable states in TaS_2 and other materials. This will allow progress in the understanding of formation and the expansion of specific CDW-phases under different tuning parameters. Images of respective phases on a smaller length scale require methods operating at higher resolution as elaborated below.

4.3. Photo-Assisted Scanning Tunneling Microscopy

Defects and atomic-scale phenomena, such as strain, vacancies, or phase boundaries play a significant role in altering the material's electronic structure, thereby influencing phase transitions.[151,152] The atomic resolution of STM allows these local changes to be directly visualized, enabling a deeper understanding of these processes and their influence on the macroscopic properties of materials. Scanning tunneling microscopy (STM) combined with laser excitation has proven to be a powerful experimental method to study non-equilibrium properties of materials at atomic resolution.[91,153,154]

We demonstrate its potential by studies of electronic phase transition in TaS_2,[155,156] where optical excitations can change the electronic and structural properties.[157–159] The crystals are grown up to millimeter sizes and can be exfoliated in UHV, making it an ideal case study for STM-based studies. By combining STM with laser excitation (**Figure 12a**)), we can trigger phase transitions in TaS_2 at localized regions, enabling the study its dynamics at the atomic level. Unfortunately, this capability comes with many challenges, which have been addressed over the last decade.[91,160] To improve the stability and lateral resolution of the excitation, optical antennas, and active beam line stabilization by image recognition were developed, in order to reach sub-Ångstrøm resolution.[89] This can provide valuable information on the effect of local defects on phase transitions.

The commensurate charge density wave (CDW) of 1T-TaS_2 at low temperatures (<180 K) is formed by 12 Tantalum atoms being slightly displaced toward a central Ta atom, forming a star-like configuration (Figure 12b)[157,159] The resulting $\sqrt{13}\times\sqrt{13}R13.9°$-reconstruction shows long range order but can be broken up into many small domains by defects, electronic or optical pumping.[152,158,161] Figure 12c–e shows STM topographies of a formerly homogeneously reconstructed area (c), which broke up into several domains, after a single intense laser pulse (d and e). As indicated by the lines in d, the rotational degree of freedom resulted in domains with different relative orientations (R+13.9° and R-13.9°), giving rise to chirality, which cannot be observed under equlibrium conditions. By zooming out, one can see that

the laser also has induced a whole zoo of other domain boundaries and defects calling for further investigation. (s. Figure 12e) Apart from their orientation, the domains can differ in their electronic properties, which can also be accessed in an STM by utilizing Scanning Tunneling Spectroscopy (STS). Combining STM with laser excitation provides a powerful approach to study these different domains and investigate their properties one by one with a high level of detail. The technique's ability to provide insight into the roles of local defects and atomic-scale phenomena should open up new avenues for scientific investigation.[89,158,162]

4.4. Ultrafast Transmission Electron Microscopy (UTEM)

Energy conversion naturally entails non-equilibrium processes that rely on the coupling of different microscopic degrees of freedom. The strengths and hierarchies of the interactions among electronic, lattice, and spin degrees motivate ultrafast spatiotemporal measurements to access the dynamical evolution of excitations and the nanoscale flow of energy in phase transitions.

Ultrafast Transmission Electron Microscopy (UTEM) is an emerging technique that combines the versatile imaging, diffraction, and spectroscopy capabilities of electron microscopes with the ultimate temporal resolution provided by laser spectroscopy. In this approach, transient states of matter and dynamical processes on the femtosecond timescale can be observed in a laser-pump, electron-probe scheme: In a prototypical UTEM experiment, electronic excitation by a short laser pulse induces a structural response that is probed by electron pulses at a variable delay. Highest spatial and temporal resolution is achieved for reversible processes that can be probed stroboscopically, using only about one electron per pulse. In contrast, irreversible changes require single-shot imaging with a large number of electrons in a single pulse, an approach termed Dynamical TEM (DTEM) for differentiation, which severely affects spatiotemporal resolutions.

In the development of ultrafast electron microscopy, groundbreaking research at the Technical University Berlin,[163] Caltech,[164] and Lawrence Livermore National Labs[165] showed the potential of pump-probe imaging in both stroboscopic[166] and single-shot operation.[167] These works employed planar photocathodes, which limits both spatial coherence and temporal resolution. In order the enhance the quality of the pulsed electron beam, to increase achievable temporal resolution, and to leverage the abilities of modern TEMs on ultrafast timescales, laser-triggered field emitters were introduced in the Göttingen UTEM.[168,169] Enabled by continuing developments, in recent years, time-resolved electron microscopy has been experiencing rapid growth in performance and breadth of applications, spanning ultrafast magnetization dynamics,[170–172] strain-wave excitation and propagation,[173–175] and structural phase transformations[127,176] with reviews found in Refs. [177–181]

To illustrate the capabilities of UTEM in addressing highly relevant questions in energy conversion and tunable materials, we discuss the probing of a light-induced structural phase transition[127] in the prototypical charge-density wave (CDW) material 1*T*-TaS_2. Owing to its strong electron-phonon and electron-electron interactions as well as reduced dimensionality, the phase diagram of this material features a sequence of CDW phases coupled to a periodic lattice distortion.[182] Transitions among these phases were the subject of ultrafast diffraction experiments in the past.[183–189]

Figure 13 displays the experimental scheme and observation of the transformation between the semi-metallic, nearly-commensurate (NC) and the metallic incommensurate (IC) CDW phase of 1*T*-TaS_2, with combined 5-nm spatial and femtosecond temporal resolutions.[127] In this experiment, sensitivity to local changes of the CDW-coupled periodic lattice distortion is obtained by a tailor-made dark-field mask (Figure 13b). The mask transmits only electrons that have undergone scattering by the NC-CDW periodicity, which are evident as satellite peaks in the diffraction pattern (Figure 13c,d). With the DF mask inserted, the produced real-space dark-field image is a direct representation of the structural order parameter, i.e., the amplitude of the lattice distortion (Figure 13e) which can be imaged as a function of time. In particular, the global quench of the NC CDW amplitude 0.75 ps after laser excitation is observed across the field-of-view (Figure 13e). Within the first few picoseconds, a spatially inhomogeneous recovery of the NC PLD amplitude is observed which reflects the approximately four-fold symmetric excitation profile on the sample (Figure 13f). At a delay of 130 ps, a clear phase separation is evident, followed by a continuous shrinkage of the phase-switched areas on the nanosecond timescale. Interestingly, the ultrafast response of the material to femtosecond excitation is in stark contrast to inducing the phase transition via continuous-wave laser excitation, where a single domain originating in the center of the thin-film, growing with increasing excitation density, is found.[127]

The above observations, corroborated by Ginzburg-Landau simulations, evidence rapid hot-electron transport into the sample, illustrate the timescale of phase boundary formation and elucidate non-equilibrium structural relaxation. The underlying contrast enhancement is readily transferrable to other geometries and materials, providing a pathway to in situ and ultrafast imaging of the correlation between non-equilibrium responses and phase transformations, heterogeneity, and microstructure.

5. Atomic Scale and Quantum Studies of Dynamic Interfaces in Reactive States

Interfaces are the most relevant sites, where chemical reactions happen and can be controlled. In particular, aqueous interfaces play an important role for catalysis and electro- or photochemical processes. Despite of many decades of research, the atomic and electronic structure and dynamics of such interfaces in reactive states are only insufficiently captured.[190] This is even true for equilibrium states, such as electric double layers.[191] During catalysis, the possible development of spatio-temporal patterns at surfaces is known since the 1990's.[192] However, the necessary further development into atomic-scale studies of (dynamic) active site(s),[193] i.e., atoms, defects, or collective entities where reactions happen,[28] has become feasible only recently. This became possible, via advancing in situ environmental transmission electron microscopy (ETEM) to image dynamic active sites under reactive conditions in real space as well as grazing incidence in situ and time-resolved X-ray spectroscopy methods, such as resonant inelastic X-ray scattering (RIXS) to study occupied and unoccupied electron states of reactive surfaces.

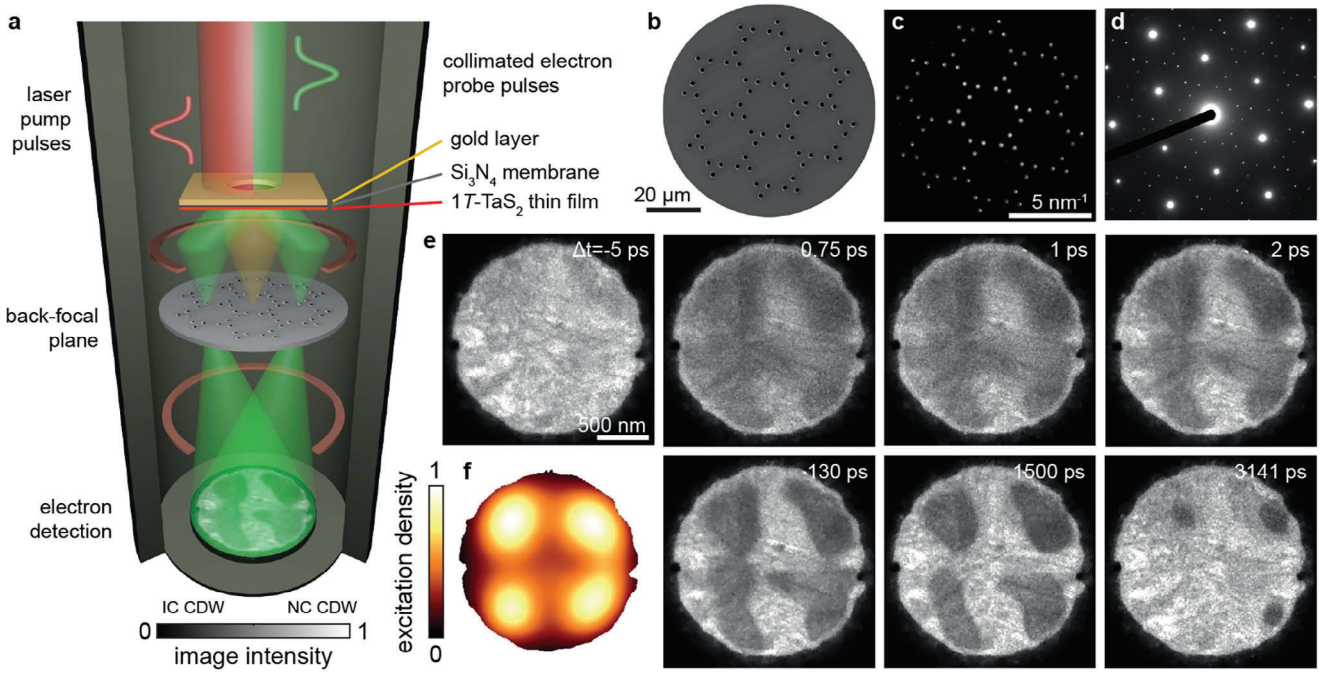

Figure 13. a) Selective contrast enhancement in an ultrafast transmission electron microscope by an analog Fourier filter placed in the back-focal plane of the objective lens. b) Dark-field aperture array. c,d) Aligning the aperture array to the electron diffractogram of the NC CDW/PLD phase of 1T-TaS_2 filters electrons diffracted by the PLD. e,f) The tailored DF imaging allows to follow the structural transformation from the NC (bright contrast) into the IC phase (dark) as induced by a spatially structured excitation. The IC domain nucleation and growth and dynamics at interphase boundaries are resolved with combined 5-nm spatial and sub-500-fs temporal resolution. From reference,[127] reprinted with permission from AAAS, copyright 2021.

An atomic-scale understanding of electrochemical double layers requires the understanding of the atomic-scale electric field drop at the interface, including the rich variety of dynamical structures of dipole water layers at surfaces that can occur due to the subtle balance of competing water–surface and water–water interactions with similar strength.[194] Since the structure of water affects the chemical coordination and bonding of adsorbates, transport of ions, local electric fields and can even influence the defect formation and dynamic structure of the solid interface, experimental access is highly desirable. However, the study of solid–liquid and other buried interfaces at atomic scale is notoriously difficult with many of the traditional surface- characterization techniques.[195] Progress of in situ electron off-axis electron holography with Ångstrøm spatial resolution at interface to absorbed water now gives unique insights into that topic exploiting the effect of atomic electric potentials on the electron wave.[196] This is all the more necessary because theoretical modeling is very challenging[27] and is thus often limited to idealizations. Feedback from atomic scale experimental studies is thus required.

Furthermore, a fundamental issue in understanding reactivity at interfaces is the impact of quantum dynamics. Although all chemical processes implicitly depend on the quantum nature of matter, detecting explicit quantum effects in chemical energy conversion is a major challenge.[197] In many cases, chemical reactions are described in terms of classical motion of atoms on an energy potential surface, which is determined by the electronic structure of the system. Such a decoupling from the structural dynamics is called Born-Oppenheimer approximation. However, its validity and limits are currently one of the most challenging topics in surface chemistry.[198] For example, quantum effects are visible in the coherent structural dynamics of atoms or molecules coupled to infrared optical excitations, now accessible via infrared spectroscopy that achieves single photon detection efficiency. The impact of quantum dynamics in chemical reactivity is presently in many cases beyond current knowledge.[199] **Figure 14** gives an overview of some of the fundamental atomic-scale processes that are involved in chemical reactivity at interfaces and which are discussed in this chapter.

5.1. Transporting and Concentrating Vibrational Energy to Promote Isomerization

Infrared spectroscopy is one of the most powerful tools in molecular science, as spectral lines provide fingerprints for specific molecules – even specific bonds in molecules – that can be incredibly useful for analyzing molecular dynamics of chemical reactions. Infrared emission spectroscopy has been revolutionized by the development of superconducting photon detectors, which have been recently reviewed.[200] In Göttingen, we have developed an infrared emission spectrometer employing a scanning liquid nitrogen-cooled monochromator and a single photon superconducting nanowire detector (SNSPD)[37] that has enabled many new experiments to be carried out with the aim to understand low-temperature quantum dynamics of chemical reactions. Some highlights from this effort include: i) the discovery of vibrational relaxation of molecules at surfaces that does not

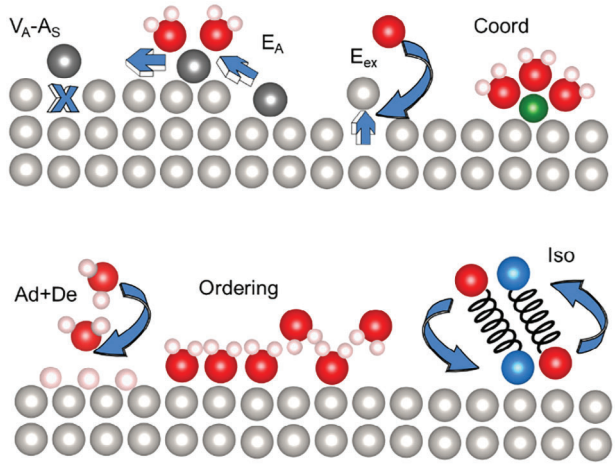

Figure 14. Schematic representation of fundamental atomic scale and quantum processes at buried and aqueous interfaces that can be involved in chemical reactivity. Top row: Vacancy-adatom pair formation V_A-A_S, thermally activated adatom hopping with barrier E_A, modified by steps and partial solvation, ion exchange processes with energy E_{ex}; solvated adatom with modified coordination. Bottom row: Adsorption and desorption (Ad+De) of molecules (e.g. water), depending on surface termination; formation of ordered mono or bilayers of water (Ordering) with different hydrogen down or up configurations as part of the electric double layer. Vibrational energy transfer at interfaces depends on surface isomerization (Iso) and affects infrared photochemistry.

depend on the interatomic forces, but rather on electromagnetic interactions;[201] ii) the discovery of up-side-down molecules at a surface[202] and iii) the observation of condensed phase resonance enhanced heavy atom tunneling.[203]

Figure 15 shows a recent realization of an artificial energy harvesting system operating with vibrational energy that was made possible by the advances in emission spectroscopy provided by the SNSPD.[204] It shows that directional control of vibrational energy transport at interfaces provides new possibilities for driving surface reactions as well as for harvesting photons in the mid-infrared range by vibration-to-vibration (V-V) energy transfer, which behaves in many ways like Förster resonance energy transfer (FRET).[205–207] Such a process allows extending light harvesting further to the mid-infrared, where suitable low-energy electronic transitions are unavailable.

5.2. Accessing the Inner Helmholtz Layer at Electrode Surfaces by In Situ Electron Holography

The theoretical concept of an electrochemical double layer that forms between a solid surface and adsorbed molecules as a result of electron transfer in equilibrium was introduced by Helmholtz in 1879.[208] The model was later extended by Gouy[209] and Chapman[210] as well as by Stern[211] by considering an inner layer of adsorbed ions and the outer space charge layer built by a gradient of diffusing ions. However, even after 100 years, it remains an unparalleled challenge to access the structure of the electric double layer.[191] Simple geometrical models of two layers as suggested by the pioneers cannot provide quantitative agreement with electrochemical spectroscopy. Despite the insight into laterally ordered water layers on metal surfaces provided by scanning tunneling experiments at low temperatures[212] and room-temperature transversal order on chalcogenides and oxides obtained by 3D AFM,[213] there is a gap in the clarification of the atomic and electric field dynamic structure of the electric double layer at room temperature. Modern insights are mainly based on molecular dynamics and density functional theory.[214] Spectroscopic experiments can only indirectly access the orientation of water dipoles by interpretation of chemical information obtained by ab initio molecular dynamics.[215,216] Confirmation of the ordered dipole layer at room temperature in real space at the atomic level was still pending.

Recently, off-axis electron holography was developed to a level that allows the reconstruction of the phase of the object wave with 1Å spatial resolution and a high sensitivity of phase measurement of $2\pi/452$.[196] Based on phase-shifting electron holography as proposed by Ru et al.,[217] this method allows the application of electron holography in transmission electron microscopes dedicated to in situ studies and hence typically equipped with a single biprism. The achieved spatial resolution is sufficient to enable the reconstruction of the object wave over the complete spatial frequency domain up to atomic resolution and thus study projected atomic potentials as well as space charge layers. A key step was considering the effect of biprism- and sample drift in the recorded hologram series and developing an appropriate correction scheme.

Figure 16 summarizes the key steps toward real-space imaging of the electric double layer at the Pt (111) interface to H_2O. Figure 16a–c shows the theoretical results on the structure of an ideal flat interface and a perfect surface based on molecular dynamics (Figure 16a) and the resulting phase of the electron wave (Figure 16b,c) as obtained from image simulations. Figure 16d,e reveals the measured electron phase shifts at the cross-section of a Pt (111) interface in high vacuum by means of phase-shifting electron holography. Naturally, the H_2O dipoles are absent in such an experiment. Performing the same experiments in situ in H_2O at different electric potentials establishes the presence of two monolayers of ordered H_2O molecules that change their orientation upon biasing.[218] Since the electron phase shift at atomic resolution is a measure of the projected electric potentials, this experiment gives access to the time-averaged spatial structure of the oscillating electric dipole field on atomic scales and its change under electric polarization.

Even though, MRSTEM and PS-EH are complementary techniques in that they follow different electron-optical arrangements and measure different quantities, i.e., the gradient of the projected electrostatic potential in the case of MRSTEM and the projected electrostatic potential in the case of PS-EH, their range of applications is very similar. A detailed comparison of the concepts of MRSTEM and standard EH is given in Ref. [63]. From a practical point of view, the much lower dose rate of PS-EH compared to the focused probe used in MRSTEM can be beneficial, in particular for beam-sensitive materials and to avoid contamination. We note, however, that the accumulated dose of PS-EH series typically exceeds that of MRSTEM and that current development of detectors[219] promises further progress.

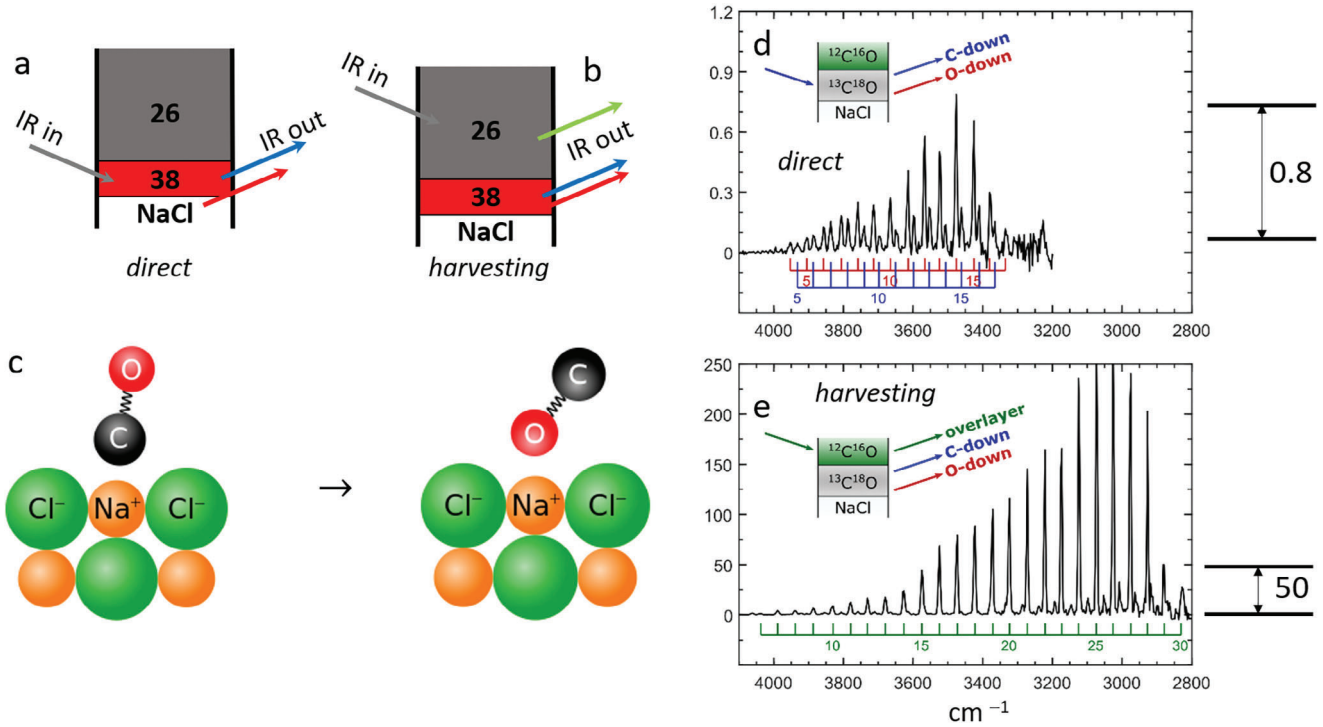

Figure 15. Infrared Light harvesting: a monolayer of $^{13}C^{18}O$ (38) lies buried beneath ≈ 100 molecular layers of $^{12}C^{16}O$ (26). a) Direct excitation of molecules at the interface. b) Light-harvesting concept: an infrared laser excites the overlayer and the resulting vibrational quanta are transported to the monolayer at the interface. The vibrational energy appearing at the interface induces an isomerization reaction c) producing an up-side-down CO molecule at the interface. d) Shows the infrared emission spectra obtained when the monolayer is excited directly. Emission lines from the up-side down CO are shown with the red comb. e) Shows the emission spectrum obtained when exciting the overlayer. Mainly emission comes from the overlayer (green comb) but extra lines appear (not labeled) some of which arise from the up-side-down CO molecule at the interface. The molecule is flipped upside down about 30x more efficiently using the harvesting approach compared to direct excitation.[204]

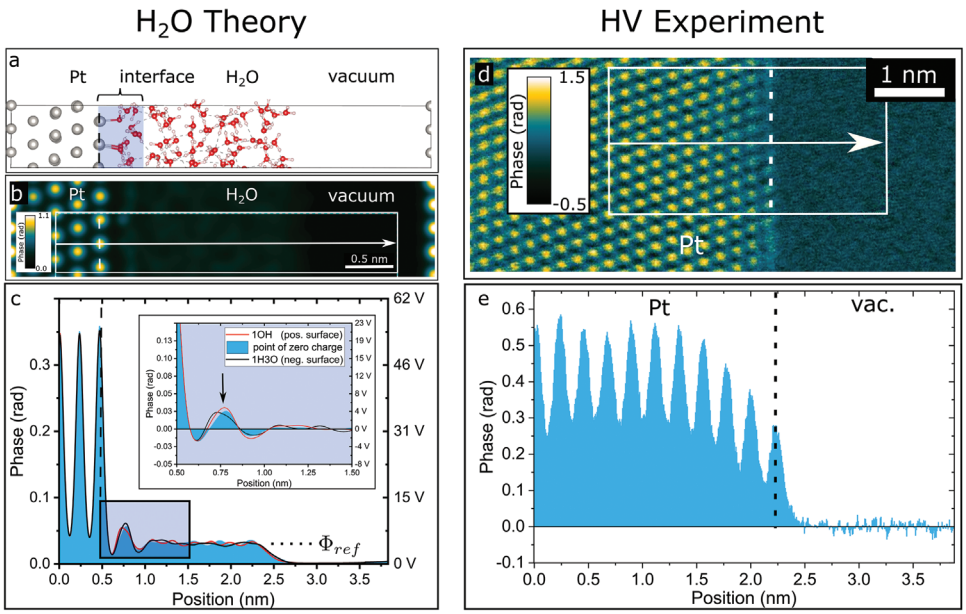

Figure 16. Study of the electric double layer at Pt (111) surface by using in situ electron holography. a) Structural model of the perfect idealized interface as revealed by molecular dynamics and b,c) calculated electron phase shift for a thin Pt lamella in [110] zone axis, revealing two layers of ordered H_2O dipoles which can be detected as an electron phase oscillation. d) Experimental electron phase of a thin Pt lamella with same orientation and thickness in high vacuum (HV), where the H_2O layer is absent. e) Profile of the electron phase showing oscillations due to the mapping of the projected atomic potentials of the Pt columns, which decreases toward the surface due to a thickness gradient.[218]

5.3. High-Resolution Imaging of Atomic Surface Processes at Perovskite Oxide Electrodes in Water Using Environmental TEM

Electrochemical activity and stability of electrodes can be strongly affected by interfacial electrolyte interactions that are accompanied by dramatic changes of structure and dynamics of interfaces. Here, the distinction between reversible dynamics that emerge in a stationary state and irreversible processes that change the activity is essential. Such insights are promoted by the progress of *in-operando* studies that can address different types of dynamical changes, including (i) the rather slow formation of the active state of the electrode surface during potential cycling;[220–222] (ii) a rather fast reversible interface dynamics due electrolyte-induced changes of thermally activated mobility of surface atoms[223] or adatoms.[224] For example, it is suggested that non-equilibrium dynamics of catalyst atoms are involved in OER mechanism.[225] Finally, (iii) we mention surface dynamics of irreversible defect reactions, as, e.g., oxygen vacancy formation[226,227] or the dissolution of metallic species[228] that lead to gradual degradation even for highest performance systems such as RuO_2.[229]

In situ, environmental transmission electron microscopy (ETEM) in combination with aberration- correction and image simulation has developed to a level, where it can provide atomic resolution real-space information about the structure of interfaces under reactive conditions. This involves the study of equilibrium surface reconstruction in various ambient conditions,[230–232] including strategies for controlling the impact of electron beams.[233,234] Control of the applied electric potential at TEM samples enables in situ studies of electrode surfaces in ETEM under anodic polarization, approaching OER-relevant potentials.[235]

Figure 17 shows interface dynamics of three catalytically active complex oxides under catalytic conditions, i.e., during the oxygen evolution reaction (OER) and the water shift reaction. The active site at the TiO_2 (001) surface consists of the dynamic twin protrusions at the Ti ridges (blue arrows in Figure 17c) on the (1 × 4) reconstructed (001) surface. This site can absorb water as well as OH dissociatively, which are possible intermediate steps in oxygen evolution as well as water gas shift reactions.[236] The active site of the $La_{0.6}Sr_{0.4}MnO_3$ (001) surface consists of dynamic Mn adatoms on a stable A-site terminated surface (Figure 17d–f).[237] It shows thermally activated surface hopping with a hopping rate that is >20x faster than in high vacuum or oxygen environments. This is explained in terms of partial solvation of Mn in H_2O and leads to a modified coordination chemistry in the OER. Similar results are found at the interface of a cobaltite perovskite to H_2O, where the enhanced Co-mobility appears in conjugation with the formation of a surface hydroxide.[238]

In contrast to the mobile adatoms at the surface of manganite perovskite oxides, a remarkable ≈1 nm thick dynamic surface layer develops at layered partially disordered Ca-birnessite in water. Figure 17g shows the dynamic layer in 100 Pa H_2O which is absent in 100 Pa O_2 (Figure 17h).[239] The level of dynamics is stationary over at least several minutes and no degradation of the surface is visible. Such a dynamic thick subsurface layer could represent a mechanism that allows cation exchange observed during OER in phosphate buffers[240] and is interpreted as a key mechanism for electrode stabilization and electron-coupled proton transport.

5.4. Studying Site Sensitive Electronic Surface States During Water Adsorption and Splitting by In Situ and Time-Resolved Grazing Incidence Soft X-Ray Spectroscopy

The oxygen evolution reaction is a four-step electron and proton transfer reaction that forms molecular oxygen O_2 and 4 protons out of two H_2O molecules. Due to the complexity of the reaction, neither the catalytic mechanism nor the involved active sites, adsorbates, and charge transfer steps are fully understood, in particular for highly active and stable perovskite oxides. X-ray spectroscopy enables the tracking and characterization of element-sensitive and OER-specific newly formed adsorbates, charge transfer species, and intermediates as well as changes in the oxidation state of the active sites as they are dynamically formed on such catalytic perovskite's surfaces. Furthermore, the method allows to monitor effects due to defect formation.[29,241] In homogeneous catalysis research, the combination of liquid-jet technology with ultrafast high-resolution, multidimensional soft X-ray spectroscopy at synchrotrons as well as free-electron lasers allowed to watch the electron redistribution and their couplings to the solvent during catalysis in real-time.[242–245] For example, when studying the ethanol-solvent-supported photo-dissociation of the $Fe(CO)_5$ catalysts, the formation of ultrafast charge-transfer intermediates between the catalysts and ethanol facilitated dissociation reactions and guided the reaction to particular product states.[242]

Combining the liquid-jet technology with surface-sensitive soft X-ray spectroscopy methods by using grazing X-ray incidence geometry with angles below 1°, extended the application of X-ray methods toward studying heterogeneous catalysis. The grazing incidence geometry limits the soft X-ray penetration to a few nanometers, allowing for enhanced surface sensitivity. Both electron acceptor (unoccupied) and electron donor (occupied) states at the surface can be investigated under in situ conditions by using X-ray absorption spectroscopy (XAS) or X-ray emission / Resonant inelastic X-ray scattering (XES/RIXS), respectively.[29]

Figure 18 shows the RIXS experimental method for investigating the surface-near electronic structure of a single crystalline epitaxial (001) oriented $La_{0.6}Sr_{0.4}MnO_3$ (x = 0.33) electrode under OER conditions. The experimental scheme was adapted to different synchrotron and FEL light sources.[246–248] Figure 18b,c presents the recorded RIXS spectra at the Mn L-edge and O K-edge for 642.8 and 528.9 eV excitation energies, respectively. The 0 eV loss energy corresponds to the elastic recombination. Figure 18b identifies mixed or intermediate Mn^{3+}/Mn^{4+} valence states of water-covered LSMO thin films.[29] Figure 18c shows the surface change of O-K edge upon water coverage in comparison to the dry surface and to the bulk. The low energy emission feature highlighted in the inset is partially quenched in intensity (Figure 18c inset) at the surface and fully quenched in H_2O. These features are related to the Mn-O-Mn e_g states which are strongly influenced by changes of the Mn coordination and Jahn-Teller distortion at the interface, in agreement with the structural observations of emergence of mobile Mn adatoms presented in Figure 17d–f. Another notable difference is the intensity

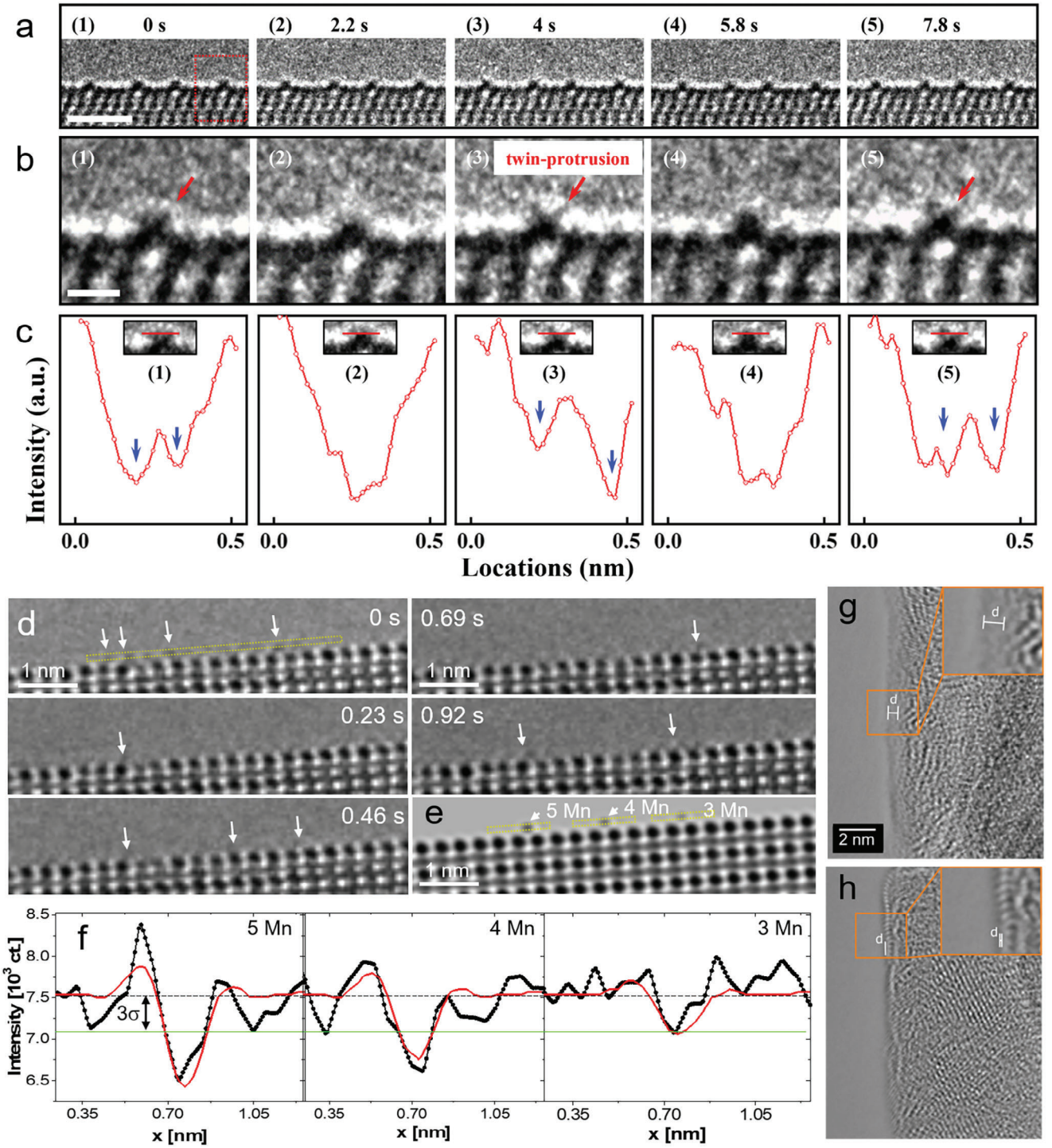

Figure 17. Reversible and stable surface dynamics of different complex oxides in H_2O vapor. a–c) Dynamic structural evolution of the (1 × 4) reconstructed (001) surface of TiO_2 in the water–gas shift reaction in CO / H_2O (1:1) vapor with pressure of 500 Pa at 700 °C. a) Sequential ETEM images, Scale bar, 2 nm. b) Enlarged ETEM images showing the dynamic structural evolution of the Ti row Scale bar, 0.5 nm. c) Intensity profiles along the lines crossed the Ti rows of b (reprinted with permission,[236] © 2020 AAAS). d–f) Dynamic Mn adatom hopping on an A-site terminated $La_{0.6}Sr_{0.4}MnO_3$ (001) surface in 0.5 Pa H_2O. d) Sequential ETEM images with appearance and disappearance of Mn atom contrast at layer surface positions. e) Image simulation reveals detection of triple or higher Mn occupancy of B-columns. f) Comparison to experimental contrast for 3, 4, and 5 Mn atoms in a column.[237] g,h) Time averaged HRTEM images of a $K_{0.2}Ca_{0.21}MnO_{2.21}$·birnessite interface to H_2O and O_2, respectively. The dynamic layer appears as a blurred image contrast of thickness of ≈ 1 nm (H_2O) and ≈0.1 nm (O_2), both at pressures of 100 Pa.[239]

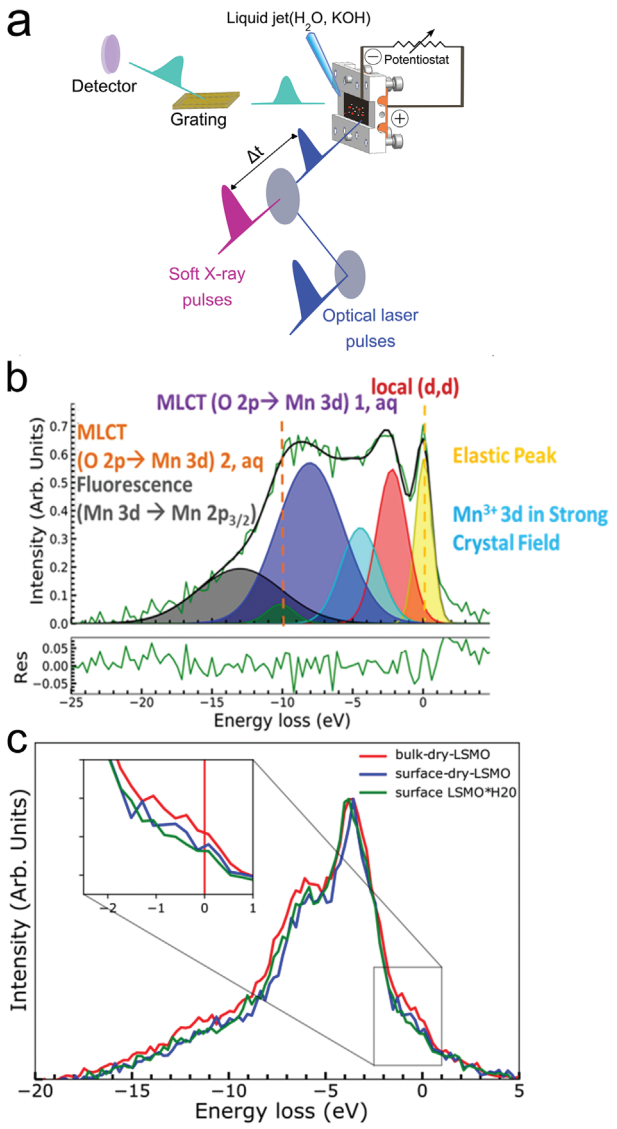

Figure 18. In situ resonant inelastic x-ray spectroscopy (RIXS) to study surface coordination at a perovskite manganese oxide $La_{0.6}Sr_{0.4}MnO_3$ (LSMO) electrode in H_2O under OER conditions. a) Sketch of the grazing incidence experimental scheme for surface-sensitive RIXS. The water-adsorbed layer on the perovskite surface was implemented by coupling the liquid jet nozzle to the sample holder. The sample holder is connected to a potentiostat to provide the required bias voltage for OER. Grazing incidence angles of <1° can be achieved for maximum surface probing. b) Mn L-edge RIXS of a water-covered LSMAO thin film electrode. The transition includes the d–d) transition and charge transfer transitions.[29] c) O K-edge RIXS of LSMO thin films for bulk (incidence angle 45°, red), surface sensitive dry (incidence angle 1° blue), and surface sensitive in water (incidence angle 1° green).

reduction of the two main O 1s peaks compared to the bulk, indicating a reduced O concentration at the surface.

6. Conclusions and open Challenges

In previous chapters, it becomes apparent that the progress in situ atomic scale methods has significantly progressed our knowledge of new and advanced energy materials, where a local understanding of complex, inhomogeneous systems or interfaces down to the atomic scale and quantum level is required. This applies to all types and steps of energy conversion, including excitations, dissipation, conversion, and energy storage. Although there has been huge progress in spatial and energy resolution of in situ methods, achieving atomic or quantum resolution is often at the limit of what can be achieved and often requires specialized and highly sophisticated equipment but also a lot of experience in applying such techniques to extract fine details.

Electromagnetic Excitations can be now studied down to single atoms or molecules, using techniques such as photo-STM, IR, and optical spectroscopy with single photon detection as well as EELS. For example, this enabled to develop an understanding of optical excitations of individual donor atoms in semiconductors and how they change their excitations in the vicinity of surfaces or space charge layers. Vibrational excitations can be steered to molecules at surfaces helping to understand their role in chemical reactivity and open pathways for IR vibrational energy harvesting. A huge step toward the atomic scale study of the effect of chemical structure and electric field on atomic and electric potential structure of interfaces and electrodes using electron holography and 4D-STEM approaches. This allows for example to develop a true understanding of the dynamical structure of the electric double layer and thus to allow proceeding toward an atomic scale understanding of electrochemical energy conversion.

The study of energy dissipation has been advanced down to the scales of individual molecules and atoms, using atomic force microscopy or inelastic surface scattering of atoms. In particular, this is an important step for the understanding of bond formation and breaking in surface chemistry as well as for the role of surface and subsurface atoms and excitations in sliding friction. In solar cells, the recombination of electrons and holes at single defects can be now studied on a nm scale using STEM-EBIC with the potential of further improvement toward the study of recombination losses at atomic scale defects such as single impurity atoms/traps. This would be particularly important for strongly correlated materials with very low screening lengths. Atomic scale energy dissipation is also involved in phase transitions. In this review, we focused on 2D materials, where nm-scale spatial inhomogeneities in the evolution of the order parameter are observed using nano-diffraction of electron probes, ultrafast TEM as well as SNOM. This progress can have a huge impact on understanding local energy conversion, e.g. in catalysis, for example with the progress in understanding and application of 2D materials.

Photovoltaic and Chemical Energy Conversion can now be studied by in situ electron microscopy methods, such as EBIC down to atomic scales. This is particularly relevant for the study of excess carrier diffusion and electron-hole separation at heterojunction interfaces and their correlation to their atomic structure. Furthermore, active sites and their dynamical behavior that control chemical energy conversion in catalysis can be imaged using environmental TEM in real space on atomic level, and single atom resolution is in reach with improved, e.g. single electron detectors. This is complemented by the huge progress of in situ x-ray spectroscopy methods, where changes in bonding, chemical coordination, and electronic correlations can be

studied on a meV energy scale. One of the major next steps could be the combination of high spatial and energy resolution, e.g., by using correlated microscopy and x-ray studies or by exploiting the amazing progress of energy resolution in electron energy loss spectroscopy in situ experiments.

In summary, our review shows that despite the significant progress, further advancing atomic scale and quantum level in situ methods is highly desired and has a high potential to resolve open questions of energy conversion in complex materials. This often starts by the improvement of specialized techniques or is often driven by need to study a specific problem and then later can spread out and used for the study a broader class of out-of-equilibrium material properties.

Acknowledgements

C.J. and M.S. contributed equally to this work. This contribution was funded by the Deutsche Forschungsgemeinschaft (DFG, German Research Foundation) 217133147/SFB 1073, projects A01, A04, A05, B02, C02, C04, and Z02. The authors would like to thank Iniyan Sivakumar and Jörg Hoffmann for valuable support.

Open access funding enabled and organized by Projekt DEAL.

Conflict of Interest

The authors declare no conflict of interest.

Keywords

energy materials, high-resolution, in situ methods, photovoltaics, surface chemistry

Received: September 18, 2024
Revised: December 17, 2024
Published online: February 3, 2025

[1] C. Ballif, F.-J. Haug, M. Boccard, P. J. Verlinden, G. Hahn, *Nat. Rev. Mater.* **2022**, *7*, 8597.
[2] M. Chatenet, B. G. Pollet, D. R. Dekel, F. Dionigi, J. Deseure, P. Millet, R. D. Braatz, M. Z. Bazant, M. Eikerling, I. Staffell, P. Balcombe, Y. Shao-Horn, H. Schäfer, *Chem. Soc. Rev.* **2022**, *51*, 4583.
[3] S. Ji, C. Jun, Y. Chen, D. Wang, *Precis. Chem.* **2023**, *1*, 199.
[4] J. I. Pedrero, D. Martínez-López, J. Calvo-Irisarri, M. Pleguezuelos, M. B. Sánchez, A. Fernández-Sisón, *Forsc. Ingenieurwes.* **2021**, *86*, 321.
[5] National Research Council, *Condensed-Matter and Materials Physics: The Science of the World Around Us*, The National Academies Press, Washington, DC, **2007**.
[6] K. L. Schulte, J. Simon, M. A. Steiner, A. J. Ptak, *Cell Rep. Phys. Sci.* **2023**, *4*, 101541.
[7] Y. Zhou, L. M. Herz, A. K.-Y. Jen, M. Saliba, *Nat. Energy* **2022**, *7*, 794.
[8] C. Flathmann, T. Meyer, V. Titova, J. Schmidt, M. Seibt, *Sci. Rep.* **2023**, *13*, 3124.
[9] L. Ma, P. X. Nguyen, Z. Wang, Y. Zeng, K. Watanabe, T. Taniguchi, A. H. MacDonald, K. F. Mak, J. Shan, *Nature* **2021**, *598*, 585.
[10] J. Fojt, T. P. Rossi, M. Kuisma, P. Erhart, *Nano Lett.* **2022**, *22*, 8786.
[11] Y. Han, L. Wang, K. Cao, J. Zhou, Y. Zhu, Y. Hou, Y. Lu, *Chem. Rev.* **2023**, *123*, 14119.
[12] M. Mecklenburg, W. A. Hubbard, J. J. Lodico, B. Regan, *Ultramicroscopy* **2019**, *207*, 112852.
[13] K. Teichmann, M. Wenderoth, S. Loth, J. K. Garleff, A. P. Wijnheijmer, P. M. Koenraad, R. G. Ulbrich, *Nano Lett.* **2011**, *11*, 3538.
[14] E. P. Smakman, P. L. J. Helgers, J. Verheyen, P. M. Koenraad, R. Möller, *Phys. Rev. B* **2014**, *90*, 4.
[15] S. P. Rittmeyer, V. J. Bukas, K. Reuter, *Adv. Phys.* **2017**, *3*, 1381574.
[16] J. Neugebohren, D. Borodin, H. W. Hahn, J. Altschäffel, A. Kandratsenka, D. J. Auerbach, C. T. Campbell, D. Schwarzer, D. J. Harding, A. M. Wodtke, T. N. Kitsopoulos, *Nature* **2018**, *558*, 280.
[17] M. N. R. Ashfold, K. Yuan, X. Yang, *J. Chem. Phys.* **2018**, *149*, 8.
[18] J. Y. Park, M. Salmeron, *Chem. Rev.* **2013**, *114*, 677.
[19] Z.-G. Li, M. Zacharias, Y. Zhang, F. Wei, Y. Qin, Y.-Q. Yang, L.-C. An, F.-F. Gao, W. Li, J. Even, X.-H. Bu, *ACS Energy Lett.* **2023**, *8*, 3016.
[20] S. Rajpurohit, J. Simoni, L. Z. Tan, *Nanoscale Adv.* **2022**, *4*, 4997.
[21] W. Li, X. Qian, J. Li, *Nat. Rev. Mater.* **2021**, *6*, 829.
[22] H. Wu, L. Li, L.-Z. Liang, S. Liang, Y.-Y. Zhu, X.-H. Zhu, *J. Eur. Ceram. Soc.* **2015**, *35*, 411.
[23] L. Yu, B. M. Hudak, A. Ullah, M. P. Thomas, C. C. Porter, A. Thisera, R. H. Pham, M. De Alwis Goonatilleke, B. S. Guiton, *Chem. Mater.* **2020**, *32*, 639.
[24] J. M. Atkin, S. Berweger, A. C. Jones, M. B. Raschke, *Adv. Phys.* **2012**, *61*, 745.
[25] D. Filippetto, P. Musumeci, R. Li, B. Siwick, M. Otto, M. Centurion, J. Nunes, *Rev. Mod. Phys.* **2022**, *94*, 045004.
[26] M. F. Ruiz-Lopez, J. S. Francisco, M. T. C. Martins-Costa, J. M. Anglada, *Nat. Rev. Chem.* **2020**, *4*, 459.
[27] A. Gros, S. Sakong, *Chem. Rev.* **2022**, *122*, 10746.
[28] C. Vogt, B. M. Weckhuysen, *Nat. Rev. Chem.* **2022**, *6*, 89.
[29] T. Reuss, S. S. Nair Lalithambika, C. David, F. Döring, C. Jooss, M. Risch, S. Techert, *Acc. Chem. Res.* **2023**, *56*, 203.
[30] P. L. Gai, R. Sharma, F. M. Ross, *MRS Bull.* **2008**, *33*, 107.
[31] J. R. Jinschek, *Chem. Commun.* **2014**, *50*, 2696.
[32] J. Qu, M. Sui, R. Li, *iScience* **2023**, *26*, 107072.
[33] M. Salmeron, B. Eren, *Chem. Rev.* **2020**, *121*, 962.
[34] M. van Spronsen, G. van Baarle, C. Herbschleb, J. Frenken, I. Groot, *Catal. Today* **2015**, *244*, 85.
[35] J. Kim, Y. Yu, T. W. Go, J.-J. Gallet, F. Bournel, B. S. Mun, J. Y. Park, *Nat. Commun.* **2023**, *14*, 3273.
[36] A. M. Wodtke, D. Matsiev, D. J. Auerbach, *Prog. Surf. Sci.* **2008**, *83*, 167.
[37] L. Chen, D. Schwarzer, J. A. Lau, V. B. Verma, M. J. Stevens, F. Marsili, R. P. Mirin, S. W. Nam, A. M. Wodtke, *Opt. Express* **2018**, *26*, 14859.
[38] W. Shockley, H. J. Queisser, *J. Appl. Phys.* **1961**, *32*, 510.
[39] M. Yamaguchi, F. Dimroth, J. F. Geisz, N. J. Ekins-Daukes, *J. Appl. Phys.* **2021**, *129*, 24.
[40] M. A. Green, *Third Generation Photovoltaics*, Springer Series in Photonics. Springer, Berlin, Heidelberg **2003**.
[41] A. Pandikumar, G. Murugadoss, *Third Generation Photovoltaic Technology*, Materials Research Forum LLC, Millersville (PA) **2024**.
[42] B. Kressdorf, T. Meyer, A. Belenchuk, O. Shapoval, M. ten Brink, S. Melles, U. Ross, J. Hoffmann, V. Moshnyaga, M. Seibt, P. Blöchl, C. Jooss, *Phys. Rev. Appl.* **2020**, *14*, 054006.
[43] P. Peretzki, B. Ifland, C. Jooss, M. Seibt, *Physica Status Solidi RRL* **2017**, *11*, 1600358.
[44] P. Würfel, T. Trupke, T. Puzzer, E. Schäffer, W. Warta, S. W. Glunz, *J. Appl. Phys.* **2007**, *101*, 12.
[45] C. Flathmann, *Ph.D. thesis*, University of Goettingen, **2023**.
[46] M. Vatanparast, R. Egoavil, T. W. Reenaas, J. Verbeeck, R. Holmestad, P. E. Vullum, *Ultramicroscopy* **2017**, *182*, 92.
[47] M. Stöger-Pollach, H. Franco, P. Schattschneider, S. Lazar, B. Schaffer, W. Grogger, H. Zandbergen, *Micron* **2006**, *37*, 396.
[48] S. Martí-Sánchez, M. Botifoll, E. Oksenberg, C. Koch, C. Borja, M. C. Spadaro, V. Di Giulio, Q. Ramasse, F. J. García de Abajo, E. Joselevich, J. Arbiol, *Nat. Commun.* **2022**, *13*, 1.

[49] S. Korneychuk, B. Partoens, G. Guzzinati, R. Ramaneti, J. Derluyn, K. Haenen, J. Verbeeck, *Ultramicroscopy* **2018**, *189*, 76.
[50] G. Saucke, J. Norpoth, C. Jooss, D. Su, Y. Zhu, *Phys. Rev. B* **2012**, *85*, 165315.
[51] V. J. Keast, A. J. Scott, R. Brydson, D. B. Williams, J. Bruley, *J. Microsc.* **2001**, *203*, 135.
[52] D. Raiser, S. Mildner, B. Ifland, M. Sotoudeh, P. Blöchl, S. Techert, C. Jooss, *Adv. Energy Mater.* **2017**, *7*, 12.
[53] S. Frabboni, G. Matteucci, G. Pozzi, M. Vanzi, *Phys. Rev. Lett.* **1985**, *55*, 2196.
[54] M. R. McCartney, D. J. Smith, R. Hull, J. C. Bean, E. Voelkl, B. Frost, *Appl. Phys. Lett.* **1994**, *65*, 2603.
[55] W. D. Rau, P. Schwander, F. H. Baumann, W. Höppner, A. Ourmazd, *Phys. Rev. Lett.* **1999**, *82*, 2614.
[56] A. C. Twitchett, R. E. DuninBorkowski, P. A. Midgley, *Phys. Rev. Lett.* **2002**, *88*, 238302.
[57] M. Beleggia, P. F. Fazzini, P. Merli, G. Pozzi, *Phys. Rev. B* **2003**, *67*, 4.
[58] D. Cooper, C. Licitra, Y. Boussadi, B. Ben-Bakir, B. Masenelli, *Small Methods* **2023**, *7*, 9.
[59] D. Cooper, V. Boureau, *Microsc. Microanal.* **2024**, *30*.
[60] N. Shibata, S. D. Findlay, Y. Kohno, H. Sawada, Y. Kondo, Y. Ikuhara, *Nat. Phys.* **2012**, *8*, 611.
[61] H. Rose, *Ultramicroscopy* **1976**, *2*, 251.
[62] K. Müller, F. F. Krause, A. Béché, M. Schowalter, V. Galioit, S. Löffler, J. Verbeeck, J. Zweck, P. Schattschneider, A. Rosenauer, *Nat. Commun.* **2014**, *5*, 5653.
[63] F. Winkler, J. Barthel, R. E. Dunin-Borkowski, K. Müller-Caspary, *Ultramicroscopy* **2020**, *210*, 112926.
[64] K. Müller-Caspary, F. F. Krause, T. Grieb, S. Löffler, M. Schowalter, A. Béché, V. Galioit, D. Marquardt, J. Zweck, P. Schattschneider, J. Verbeeck, A. Rosenauer, *Ultramicroscopy* **2017**, *178*, 62.
[65] J. A. Hachtel, J. C. Idrobo, M. Chi, *Adv. Struct. Chem. Imaging* **2018**, *4*, 10.
[66] B. C. da Silva, Z. Sadre Momtaz, E. Monroy, H. Okuno, J.-L. Rouviere, D. Cooper, M. I. Den Hertog, *Nano Lett.* **2022**, *22*, 9544.
[67] T. Mawson, A. Nakamura, T. Petersen, N. Shibata, H. Sasaki, D. Paganin, M. Morgan, S. Findlay, *Ultramicroscopy* **2020**, *219*, 113097.
[68] L. Bruas, V. Boureau, A. P. Conlan, S. Martinie, J.-L. Rouviere, D. Cooper, *J. Appl. Phys.* **2020**, *127*, 20.
[69] A. Beyer, M. S. Munde, S. Firoozabadi, D. Heimes, T. Grieb, A. Rosenauer, K. Müller-Caspary, K. Volz, *Nano Lett.* **2021**, *21*, 2018.
[70] V. S. Chejarla, S. Ahmed, J. Belz, J. Scheunert, A. Beyer, K. Volz, *Small Methods* **2023**, *7*, 9.
[71] L. Jastrzebski, J. Lagowski, H. C. Gatos, *Appl. Phys. Lett.* **1975**, *27*, 537.
[72] G. Oelgart, J. Fiddicke, R. Reulke, *Phys. Status Solidi.* **1981**, *66*, 283.
[73] C. Donolato, *SolidState Electron.* **1982**, 10771081.
[74] H. J. Leamy, *J. Appl. Phys.* **1982**, *53*, R51.
[75] C. Cabanel, D. Brouri, J. Y. Laval, *Eur. Phys. J. Appl. Phys.* **2006**, 107116.
[76] W. A. Hubbard, M. Mecklenburg, H. L. Chan, B. C. Regan, *Phys. Rev. Appl.* **2018**, *10*, 4.
[77] T. Meyer, B. Kressdorf, J. Lindner, P. Peretzki, V. Roddatis, C. Jooss, M. Seibt, *J. Phys.: Conf. Ser.* **2019**, *1190*, 012009.
[78] A. P. Conlan, G. Moldovan, L. Bruas, E. Monroy, D. Cooper, *J. Appl. Phys.* **2021**, *129*, 13.
[79] W. A. Hubbard, Z. Lingley, J. Theiss, S. Sitzman, T. Ayvazian, M. Brodie, B. Foran, *Appl. Phys. Lett.* **2019**, *115*, 13.
[80] E. Vlasov, A. Skorikov, A. Sánchez-Iglesias, L. M. Liz-Marzán, J. Verbeeck, S. Bals, *ACS Mater. Lett.* **2023**, *5*, 1916.
[81] O. Dyck, J. Almutlaq, D. Lingerfelt, J. L. Swett, M. P. Oxley, B. Huang, A. R. Lupini, D. Englund, S. Jesse, *Nat. Commun.* **2023**, *14*, 7550.
[82] O. Recalde-Benitez, T. Jiang, R. Winkler, Y. Ruan, A. Zintler, E. Adabifiroozjaei, A. Arzumanov, W. A. Hubbard, T. van Omme, Y. Pivak, H. H. Perez-Garza, B. C. Regan, L. Alff, P. Komissinskiy, L. Molina-Luna, *Commun. Eng.* **2023**, *2*, 83.
[83] T. Meyer, *Ph.D. thesis*, University of Goettingen, **2020**.
[84] T. Meyer, D. A. Ehrlich, P. Pichler, V. Titova, C. Flathmann, J. Schmidt, M. Seibt, *arXiv:2109.00586 [physics.app-ph]* **2021**.
[85] K. Teichmann, M. Wenderoth, S. Loth, R. G. Ulbrich, J. K. Garleff, A. P. Wijnheijmer, P. M. Koenraad, *Phys. Rev. Lett.* **2008**, *101*, 7.
[86] J. Garleff, A. Wijnheijmer, C. v. d. Enden, P. Koenraad, *Phys. Rev. B* **2011**, *84*, 7.
[87] Y. Terada, S. Yoshida, O. Takeuchi, H. Shigekawa, *J. Phys.: Condensed Matter.* **2010**, *22*, 264008.
[88] P. Kloth, T. Thias, O. Bunjes, J. von der Haar, M. Wenderoth, *Rev. Sci. Instrum.* **2016**, *87*, 12.
[89] G. A. Traeger, M. H. Teichmann, B. Schröder, M. Wenderoth, *Rev. Sci. Instrum.* **2023**, *94*, 2.
[90] P. Kloth, K. Kaiser, M. Wenderoth, *Nat. Commun.* **2016**, *7*, 10108.
[91] P. Kloth, M. Wenderoth, *Sci. Adv.* **2017**, *3*, 3.
[92] Y. Yuzhelevski, M. Yuzhelevski, G. Jung, *Rev. Sci. Instrum.* **2000**, *71*, 1681.
[93] C. T. Rettner, F. Fabre, J. Kimman, D. J. Auerbach, *Phys. Rev. Lett.* **1985**, *55*, 1904.
[94] S. Y. Krylov, J. W. M. Frenken, *Sci. Rep.* **2021**, *11*, 19964.
[95] I. Rahinov, A. Kandratsenka, T. Schäfer, P. Shirhatti, K. Golibrzuch, A. M. Wodtke, *Phys. Chem. Chem. Phys.* **2024**, *26*, 15090.
[96] O. Bünermann, A. Kandratsenka, A. M. Wodtke, *J. Phys. Chem. A* **2021**, *125*, 3059.
[97] A. J. Weymouth, O. Gretz, E. Riegel, F. J. Giessibl, *Jpn. J. Appl. Phys.* **2022**, *61*, SL0801.
[98] I. Barel, M. Urbakh, L. Jansen, A. Schirmeisen, *Phys. Rev. Lett.* **2010**, *104*, 6.
[99] M. Kisiel, E. Gnecco, U. Gysin, L. Marot, S. Rast, E. Meyer, *Nat. Mater.* **2011**, *10*, 119.
[100] Y. Qi, J. Y. Park, B. L. M. Hendriksen, D. F. Ogletree, M. Salmeron, *Phys. Rev. B* **2008**, *77*, 18.
[101] J. Y. Park, D. F. Ogletree, P. A. Thiel, M. Salmeron, *Science* **2006**, *313*, 186.
[102] J. H. Kim, D. Fu, S. Kwon, K. Liu, J. Wu, J. Y. Park, *Adv. Mater. Interfaces* **2015**, *3*, 2.
[103] W. Wang, D. Dietzel, A. Schirmeisen, *Sci. Adv.* **2020**, *6*, 12.
[104] H. Schmidt, J.-O. Krisponeit, N. Weber, K. Samwer, C. A. Volkert, *Phys. Rev. Mater.* **2020**, *4*, 11.
[105] N. A. Weber, H. Schmidt, T. Sievert, C. Jooss, F. Güthoff, V. Moshneaga, K. Samwer, M. Krüger, C. A. Volkert, *Adv. Sci.* **2021**, *8*, 8.
[106] N. A. Weber, M. Lee, F. Schönewald, L. Schüler, V. Moshnyaga, M. Krüger, C. A. Volkert, *arXiv:2210.09677 [cond-mat.mtrl-sci]*, **2022**.
[107] M. Lee, N. Weber, C. A. Volkert, M. Krüger, *Europhys. Lett.* **2023**, *142*, 46001.
[108] A. Kleyn, T. Horn, *Phys. Rep.* **1991**, *199*, 191.
[109] G. Benedek, J. Toennies, *Surf. Sci.* **1994**, *299–300*, 587.
[110] J. E. Hurst, L. Wharton, K. C. Janda, D. J. Auerbach, *J. Chem. Phys.* **1985**, *83*, 1376.
[111] L. Schnieder, K. Seekamp-Rahn, F. Liedeker, H. Steuwe, K. H. Welge, *Faraday Discuss. Chem. Soc.* **1991**, *91*, 259.
[112] O. Bünermann, H. Jiang, Y. Dorenkamp, D. J. Auerbach, A. M. Wodtke, *Rev. Sci. Instrum.* **2018**, *89*, 9.
[113] N. Hertl, A. Kandratsenka, O. Bünermann, A. M. Wodtke, *J. Phys. Chem. A* **2021**, *125*, 5745.
[114] O. Bünermann, H. Jiang, Y. Dorenkamp, A. Kandratsenka, S. M. Janke, D. J. Auerbach, A. M. Wodtke, *Science* **2015**, *350*, 1346.
[115] K. Krüger, Y. Wang, S. Tödter, F. Debbeler, A. Matveenko, N. Hertl, X. Zhou, B. Jiang, H. Guo, A. M. Wodtke, O. Bünermann, *Nat. Chem.* **2022**, *15*, 326.

[116] H. Jiang, M. Kammler, F. Ding, Y. Dorenkamp, F. R. Manby, A. M. Wodtke, T. F. Miller, A. Kandratsenka, O. Bünermann, *Science* **2019**, *364*, 379.
[117] K. Krüger, Y. Wang, L. Zhu, B. Jiang, H. Guo, A. M. Wodtke, O. Bünermann, *Nat. Sci.* **2023**, *4*, 20230019.
[118] M. Zhou, T. Higaki, G. Hu, M. Y. Sfeir, Y. Chen, D.-e. Jiang, R. Jin, *Science* **2019**, *364*, 279.
[119] M. Wuttig, N. Yamada, *Nat. Mater.* **2007**, *6*, 824.
[120] F. J. Morin, *Phys. Rev. Lett.* **1959**, *3*, 34.
[121] S. Koshihara, T. Ishikawa, Y. Okimoto, K. Onda, R. Fukaya, M. Hada, Y. Hayashi, S. Ishihara, T. Luty, *Phys. Rep.* **2022**, *942*,1.
[122] D. Landau, *Zh. Eksp. Teor. Fiz* **1937**, *7*, 19.
[123] R. Pentcheva, R. Arras, K. Otte, V. G. Ruiz, W. E. Pickett, *Philos. Trans. R. Soc., A* **2012**, *370*, 4904.
[124] S. A. Lee, H. Jeong, S. Woo, J.-Y. Hwang, S.-Y. Choi, S.-D. Kim, M. Choi, S. Roh, H. Yu, J. Hwang, S. W. Kim, W. S. Choi, *Sci. Rep.* **2016**, *6*, 23649.
[125] D. Kim, J. Pandey, J. Jeong, W. Cho, S. Lee, S. Cho, H. Yang, *Chem. Rev.* **2023**, *123*, 11230.
[126] D. Lee, H. Jeong, H. Lee, Y. Kim, J. Y. Park, *Small* **2023**, *19*, 47.
[127] T. Danz, T. Domröse, C. Ropers, *Science* **2021**, *6527*, 371.
[128] S. Cheon, T.-H. Kim, S.-H. Lee, H. W. Yeom, *Science* **2015**, *350*, 6257.
[129] X. Zheng, W. Han, K. Yang, L. W. Wong, C. S. Tsang, K. H. Lai, F. Zheng, T. Yang, S. P. Lau, T. H. Ly, M. Yang, J. Zhao, *Sci. Adv.* **2022**, *8*, 42.
[130] K. Koo, Y. Liu, Y. Cheng, Z. Cai, X. Hu, V. P. Dravid, *Chem. Mater.* **2024**, *36*, 4078.
[131] F. Ross, *Liquid Cell Electron Microscopy, Advances in Microscopy and Microanalysis*, Cambridge University Press, Cambridge **2017**.
[132] R. Ignatans, M. Ziatdinov, R. Vasudevan, M. Valleti, V. Tileli, S. V. Kalinin, *Adv. Funct. Mater.* **2022**, *32*, 23.
[133] M. Krajnak, D. McGrouther, D. Maneuski, V. O. Shea, S. McVitie, *Ultramicroscopy* **2016**, *165*, 42.
[134] J.-L. Rouviere, A. Béché, Y. Martin, T. Denneulin, D. Cooper, *Appl. Phys. Lett.* **2013**, *103*, 24.
[135] C. Ophus, *Microsc. Microanal.* **2019**, *25*, 563.
[136] R. F. Egerton, *Electron Energy Loss Spectroscopy in the Electron Microscope*, Springer, USA **2011**.
[137] T. Meyer, B. Kressdorf, V. Roddatis, J. Hoffmann, C. Jooss, M. Seibt, *Small Methods* **2021**, *5*, 9.
[138] C. Flathmann, T. Meyer, U. Ross, A. Dehning, C. Jooss, M. Seibt, *APL Mater.* **2024**, *12*, 6.
[139] B. Kressdorf, T. Meyer, M. ten Brink, C. Seick, S. Melles, N. Ottinger, T. Titze, H. Meer, A. Weisser, J. Hoffmann, S. Mathias, H. Ulrichs, D. Steil, M. Seibt, P. E. Blöchl, C. Jooss, *Phys. Rev. B* **2021**, *103*, 235122.
[140] J. Xiao, Y. Wang, H. Wang, C. D. Pemmaraju, S. Wang, P. Muscher, E. J. Sie, C. M. Nyby, T. P. Devereaux, X. Qian, X. Zhang, A. M. Lindenberg, *Nat. Phys.* **2020**, *16*, 1028.
[141] D. A. Rehn, Y. Li, E. Pop, E. J. Reed, *npj Comput. Mater.* **2018**, *4*, 2.
[142] K. Ludwiczak, E. Lacinska, J. Binder, I. Lutsyk, M. Rogala, P. Dabrowski, Z. Klusek, R. Stepniewski, A. Wysmolek, *Solid State Commun.* **2020**, *305*, 113749.
[143] W. Li, G. V. Naik, *Opt. Mater. Express* **2019**, *9*, 497.
[144] R. Inada, Y. Onuki, S. Tanuma, *Physica B+C* **1980**, *99*, 188.
[145] X. Chen, D. Hu, R. Mescall, G. You, D. N. Basov, Q. Dai, M. Liu, *Adv. Mater.* **2019**, *31*, 24.
[146] A. J. Frenzel, A. S. McLeod, D. Z.-R. Wang, Y. Liu, W. Lu, G. Ni, A. W. Tsen, Y. Sun, A. N. Pasupathy, D. N. Basov, *Phys. Rev. B* **2018**, *97*, 3.
[147] A. Thompson, R. Gamble, J. Revelli, *Solid State Commun.* **1971**, *9*, 981.
[148] A. K. Geremew, S. Rumyantsev, F. Kargar, B. Debnath, A. Nosek, M. A. Bloodgood, M. Bockrath, T. T. Salguero, R. K. Lake, A. A. Balandin, *ACS Nano* **2019**, *13*, 7231.
[149] I. Vaskivskyi, I. A. Mihailovic, S. Brazovskii, J. Gospodaric, T. Mertelj, D. Svetin, P. Sutar, D. Mihailovic, *Nat. Commun.* **2016**, *7*, 11442.
[150] L. Stojchevska, I. Vaskivskyi, T. Mertelj, P. Kusar, D. Svetin, S. Brazovskii, D. Mihailovic, *Science* **2014**, *344*, 177.
[151] J. W. Park, J. Lee, H. W. Yeom, *npj Quantum Mater.* **2021**, *6*, 1.
[152] B. Salzmann, E. Hujala, C. Witteveen, B. Hildebrand, H. Berger, F. O. von Rohr, C. W. Nicholson, C. Monney, *Phys. Rev. Mater.* **2023**, *7*, 064005.
[153] H. Shigekawa, O. Takeuchi, M. Aoyama, *Sci. Technol. Adv. Mater.* **2005**, *6*, 582.
[154] S. Yoshida, Y. Aizawa, Z.-h. Wang, R. Oshima, Y. Mera, E. Matsuyama, H. Oigawa, O. Takeuchi, H. Shigekawa, *Nat. Nanotechnol.* **2014**, *9*, 588.
[155] Y. Yu, F. Yang, X. F. Lu, Y. J. Yan, Y.-H. Cho, L. Ma, X. Niu, S. Kim, Y.-W. Son, D. Feng, S. Li, S.-W. Cheong, X. H. Chen, Y. Zhang, *Nat. Nanotechnol.* **2015**, *10*, 270.
[156] J. Vodeb, V. V. Kabanov, Y. A. Gerasimenko, R. Venturini, J. Ravnik, M. A. van Midden, E. Zupanic, P. Sutar, D. Mihailovic, *New J. Phys.* **2019**, *21*, 083001.
[157] S. Vogelgesang, *Ph.D. thesis*, University of Goettingen, **2019**.
[158] J. Ravnik, Y. Vaskivskyi, J. Vodeb, M. Diego, R. Venturini, Y. Gerasimenko, V. Kabanov, A. Kranjec, D. Mihailovic, *Sci. Rep.* **2023**, *13*, 19622.
[159] Q. Stahl, M. Kusch, F. Heinsch, G. Garbarino, N. Kretzschmar, K. Hanff, K. Rossnagel, J. Geck, T. Ritschel, *Nat. Commun.* **2020**, *11*, 1247.
[160] Y. Terada, S. Yoshida, O. Takeuchi, H. Shigekawa, *Nat. Photonics* **2010**, *4*, 869.
[161] L. Ma, C. Ye, Y. Yu, X. F. Lu, X. Niu, S. Kim, D. Feng, D. Tom´anek, Y.-W. Son, X. H. Chen, Y. Zhang, *Nat. Commun.* **2016**, *7*, 1.
[162] B. Schröder, O. Bunjes, L. Wimmer, K. Kaiser, G. A. Traeger, T. Kotzott, C. Ropers, M. Wenderoth, *New J. Phys.* **2020**, *22*, 033047.
[163] H. Dömer, O. Bostanjoglo, *Rev. Sci. Instrum.* **2003**, *74*, 4369.
[164] A. H. Zewail, *Science* **2010**, *328*, 187.
[165] N. Browning, M. Bonds, G. Campbell, J. Evans, T. LaGrange, K. Jungjohann, D. Masiel, J. McKeown, S. Mehraeen, B. Reed, M. Santala, *Curr. Opin. Solid State Mater. Sci.* **2012**, *16*, 23.
[166] B. Barwick, H. S. Park, O.-H. Kwon, J. S. Baskin, A. H. Zewail, *Science* **2008**, *322*, 1227.
[167] J. S. Kim, T. LaGrange, B. W. Reed, M. L. Taheri, M. R. Armstrong, W. E. King, N. D. Browning, G. H. Campbell, *Science* **2008**, *321*, 1472.
[168] A. Feist, K. E. Echternkamp, J. Schauss, S. V. Yalunin, S. Schäfer, C. Ropers, *Nature* **2015**, *521*, 200.
[169] A. Feist, N. Bach, N. Rubiano da Silva, T. Danz, M. Möller, K. E. Priebe, T. Domröse, J. G. Gatzmann, S. Rost, J. Schauss, S. Strauch, R. Bormann, M. Sivis, S. Schäfer, C. Ropers, *Ultramicroscopy* **2017**, *176*, 63.
[170] N. Rubiano da Silva, M. Möller, A. Feist, H. Ulrichs, C. Ropers, S. Schäfer, *Phys. Rev. X* **2018**, *8*, 031052.
[171] M. Möller, J. H. Gaida, S. Schäfer, C. Ropers, *Commun. Phys.* **2020**, *3*, 36.
[172] G. Cao, S. Jiang, J. Akerman, J. Weissenrieder, *Nanoscale* **2021**, *13*, 3746.
[173] A. J. McKenna, J. K. Eliason, D. J. Flannigan, *Nano Lett.* **2017**, *17*, 3952.
[174] Y. Zhang, D. J. Flannigan, *Nano Lett.* **2019**, *19*, 8216.
[175] A. Feist, N. Rubiano da Silva, W. Liang, C. Ropers, S. Schäfer, *Struct. Dyn.* **2018**, *5*, 1.
[176] R. M. van der Veen, O.-H. Kwon, A. Tissot, A. Hauser, A. H. Zewail, *Nat. Chem.* **2013**, *5*, 395.
[177] W. E. King, G. H. Campbell, A. Frank, B. Reed, J. F. Schmerge, B. J. Siwick, B. C. Stuart, P. M. Weber, *J. Appl. Phys.* **2005**, *97*, 11.

[178] A. Arbouet, G. M. Caruso, F. Houdellier, *Ultrafast Transmission Electron Microscopy: Historical Development, Instrumentation, and Applications*, Elsevier, Amsterdam **2018**, pp. 1–72.
[179] A. A. Ishchenko, S. A. Aseyev, V. N. Bagratashvili, V. Y. Panchenko, E. A. Ryabov, *Phys.-Usp.* **2014**, *57*, 633.
[180] F. M. Alcorn, P. K. Jain, R. M. van der Veen, *Nat. Rev. Chem.* **2023**, *7*, 256.
[181] Y.-J. Kim, W.-W. Park, H.-W. Nho, O.-H. Kwon, *Adv. Phys: X* **2024**, *9*, 1.
[182] K. Rossnagel, *J. Phys.: Condensed Matter.* **2011**, *23*, 213001.
[183] M. Eichberger, H. Schäfer, M. Krumova, M. Beyer, J. Demsar, H. Berger, G. Moriena, G. Sciaini, R. J. D. Miller, *Nature* **2010**, *468*, 799.
[184] K. Haupt, M. Eichberger, N. Erasmus, A. Rohwer, J. Demsar, K. Rossnagel, H. Schwoerer, *Phys. Rev. Lett.* **2016**, *116*, 016402.
[185] C. Laulhé, T. Huber, G. Lantz, A. Ferrer, S. Mariager, S. Grübel, J. Rittmann, J. Johnson, V. Esposito, A. Lübcke, L. Huber, M. Kubli, M. Savoini, V. Jacques, L. Cario, B. Corraze, E. Janod, G. Ingold, P. Beaud, S. Johnson, S. Ravy, *Phys. Rev. Lett.* **2017**, *118*, 247401.
[186] L. L.e Guyader, T. Chase, A. H. Reid, R. K. Li, D. Svetin, X. Shen, T. Vecchione, X. J. Wang, D. Mihailovic, H. A. Dürr, *Struct. Dyn.* **2017**, *4*, 4.
[187] S. Vogelgesang, G. Storeck, J. G. Horstmann, T. Diekmann, M. Sivis, S. Schramm, K. Rossnagel, S. Schäfer, C. Ropers, *Nat. Phys.* **2017**, *14*, 184.
[188] A. Zong, X. Shen, A. Kogar, L. Ye, C. Marks, D. Chowdhury, T. Rohwer, B. Freelon, S. Weathersby, R. Li, J. Yang, J. Checkelsky, X. Wang, N. Gedik, *Sci. Adv.* **2018**, *4*, 10.
[189] T. Domröse, T. Danz, S. F. Schaible, K. Rossnagel, S. V. Yalunin, C. Ropers, *Nat. Mater.* **2023**, *22*, 1345.
[190] O. Björneholm, M. H. Hansen, A. Hodgson, L.-M. Liu, D. T. Limmer, A. Michaelides, P. Pedevilla, J. Rossmeisl, H. Shen, G. Tocci, E. Tyrode, M.-M. Walz, J. Werner, H. Bluhm, *Chem. Rev.* **2016**, *116*, 7698.
[191] W. Schmickler, *J. Solid State Electrochem.* **2020**, *24*, 2175.
[192] S. Jakubith, H. H. Rotermund, W. Engel, A. von Oertzen, G. Ertl, *Phys. Rev. Lett.* **1990**, *65*, 3013.
[193] F. Tao, P. A. C. Franklin, *Chem. Rev.* **2016**, *116*, 3487.
[194] A. Michaelides, A. Alavi, D. A. King, *Phys. Rev. B* **2004**, *69*, 113404.
[195] H. Shi, J. A. Lercher, X.-Y. Yu, *Catal. Sci. Technol.* **2015**, *5*, 3035.
[196] J. Lindner, U. Ross, T. Meyer, V. Boureau, M. Seibt, C. Jooss, *Ultramicroscopy* **2024**, *256*, 113880.
[197] S. A. Rice, *Procedia Chem.* **2011**, *3*, 17.
[198] A. M. Wodtke, J. C. Tully, D. J. Auerbach, *Int. Rev. Phys. Chem.* **2004**, *23*, 513.
[199] F. Gatti, B. Lasorne, H.-D. Meyer, A. Nauts, *Applications of Quantum Dynamics in Chemistry*, Springer International Publishing, London, Berlin, New York City **2017**.
[200] J. A. Lau, V. B. Verma, D. Schwarzer, A. M. Wodtke, *Chem. Soc. Rev.* **2023**, *52*, 921.
[201] L. Chen, J. A. Lau, D. Schwarzer, J. Meyer, V. B. Verma, A. M. Wodtke, *Science* **2019**, *363*, 158.
[202] J. A. Lau, A. Choudhury, C. Li, D. Schwarzer, V. B. Verma, A. M. Wodtke, *Science* **2020**, *367*, 175.
[203] A. Choudhury, J. A. DeVine, S. Sinha, J. A. Lau, A. Kandratsenka, D. Schwarzer, P. Saalfrank, A. M. Wodtke, *Nature* **2022**, *612*, 7941.
[204] J. A. Lau, L. Chen, A. Choudhury, D. Schwarzer, V. B. Verma, A. M. Wodtke, *Nature* **2021**, *589*, 391.
[205] T. Förster, *Naturwissenschaften* **1946**, *33*, 166.
[206] T. Förster, *Ann. Phys.* **1948**, *437*, 55.
[207] T. Brixner, J. Stenger, H. M. Vaswani, M. Cho, R. E. Blankenship, G. R. Fleming, *Nature* **2005**, *434*, 625.
[208] H. Helmholtz, *Ann. Phys.* **1879**, *243*, 337.
[209] M. Gouy, *J. Phys. Théorique et Appliqée* **1910**, *9*, 457.
[210] D. L. Chapman, *The London, Edinburgh, and Dublin Philosophical Magazine J. Sci.* **1913**, *25*, 475.
[211] O. Stern, *Zeitschrift für Elektrochemie und angewandte physikalische Chemie* **1924**, *30*, 508.
[212] S. Nie, P. J. Feibelman, N. C. Bartelt, K. Thürmer, *Phys. Rev. Lett.* **2010**, *105*, 026102.
[213] J. Peng, J. Guo, R. Ma, Y. Jiang, *Surf. Sci. Rep.* **2022**, *77*, 100549.
[214] S.-J. Shin, D. H. Kim, G. Bae, S. Ringe, H. Choi, H.-K. Lim, C. H. Choi, H. Kim, *Nat. Commun.* **2022**, *13*, 1.
[215] J.-J. Velasco-Velez, C. H. Wu, T. A. Pascal, L. F. Wan, J. Guo, D. Prendergast, M. Salmeron, *Science* **2014**, *346*, 831.
[216] C.-Y. Li, J.-B. Le, Y.-H. Wang, S. Chen, Z.-L. Yang, J.-F. Li, J. Cheng, Z.-Q. Tian, *Nat. Mater.* **2019**, *18*, 697.
[217] Q. Ru, G. Lai, K. Aoyama, J. Endo, A. Tonomura, *Ultramicroscopy* **1994**, *55*, 209.
[218] J. Lindner, *Ph.D. thesis*, University of Goettingen, **2024**.
[219] D. Jannis, C. Hofer, C. Gao, X. Xie, A. Béché, T. Pennycook, J. Verbeeck, *Ultramicroscopy* **2022**, *233*, 113423.
[220] R. Arrigo, M. Hävecker, M. E. Schuster, C. Ranjan, E. Stotz, A. Knop-Gericke, R. Schlögl, *Angew. Chem., Int. Ed.* **2013**, *52*, 11660.
[221] A. Bergmann, E. Martinez-Moreno, D. Teschner, P. Chernev, M. Gliech, J. F. de Araújo, T. Reier, H. Dau, P. Strasser, *Nat. Commun.* **2015**, *6*, 8625.
[222] M. Risch, F. Ringleb, M. Kohlhoff, P. Bogdanoff, P. Chernev, I. Zaharieva, H. Dau, *Energy Environ. Sci.* **2015**, *8*, 661.
[223] X. Xia, S. Xie, M. Liu, H.-C. Peng, N. Lu, J. Wang, M. J. Kim, Y. Xia, *Proc. Natl. Acad. Sci. USA* **2013**, *110*, 6669.
[224] L. Y. Chen, S. C. Ying, *Phys. Rev. B* **1994**, *49*, 13838.
[225] Y.-G. Wang, D. Mei, V.-A. Glezakou, J. Li, R. Rousseau, *Nat. Commun.* **2015**, *6*, 1.
[226] D. Mierwaldt, S. Mildner, R. Arrigo, A. Knop-Gericke, E. Franke, A. Blumenstein, J. Hoffmann, C. Jooss, *Catalysts* **2014**, *4*, 129.
[227] S. Raabe, D. Mierwaldt, J. Ciston, M. Uijttewaal, H. Stein, J. Hoffmann, Y. Zhu, P. Blöchl, C. Jooss, *Adv. Funct. Mater.* **2012**, *22*, 3378.
[228] J. Scholz, M. Risch, K. A. Stoerzinger, G. Wartner, Y. Shao-Horn, C. Jooss, *J. Phys. Chem. C* **2016**, *120*, 27746.
[229] A. Izgorodin, O. Winther-Jensen, D. R. MacFarlane, *Aust. J. Chem.* **2012**, *65*, 638.
[230] H. Yoshida, Y. Kuwauchi, J. R. Jinschek, K. Sun, S. Tanaka, M. Kohyama, S. Shimada, M. Haruta, S. Takeda, *Science* **2012**, *335*, 317.
[231] Y. Lin, Z. Wu, J. Wen, K. R. Poeppelmeier, L. D. Marks, *Nano Lett.* **2013**, *14*, 191.
[232] M. Bugnet, S. H. Overbury, Z. L. Wu, T. Epicier, *Nano Lett.* **2017**, *17*, 7652.
[233] Y. Kuwauchi, H. Yoshida, T. Akita, M. Haruta, S. Takeda, *Angew. Chem., Int. Ed.* **2012**, *51*, 7729.
[234] V. Roddatis, G. Lole, C. Jooss, *Catalysts* **2019**, *9*, 751.
[235] S. Mildner, M. Beleggia, D. Mierwaldt, T. W. Hansen, J. B. Wagner, S. Yazdi, T. Kasama, J. Ciston, Y. Zhu, C. Jooss, *J. Phys. Chem. C* **2015**, *119*, 5301.
[236] W. Yuan, B. Zhu, X.-Y. Li, T. W. Hansen, Y. Ou, K. Fang, H. Yang, Z. Zhang, J. B. Wagner, Y. Gao, Y. Wang, *Science* **2020**, *367*, 428.
[237] G. Lole, V. Roddatis, U. Ross, M. Risch, T. Meyer, L. Rump, J. Geppert, G. Wartner, P. Blöchl, C. Jooss, *Commun. Mater.* **2020**, *1*, 68.
[238] M. L. Weber, G. Lole, A. Kormanyos, A. Schwiers, L. Heymann, F. D. Speck, T. Meyer, R. Dittmann, S. Cherevko, C. Jooss, C. Baeumer, F. Gunkel, *J. Am. Chem. Soc.* **2022**, *144*, 17966.
[239] E. Ronge, J. Lindner, U. Ross, J. Melder, J. Ohms, V. Roddatis, P. Kurz, C. Jooss, *J. Phys. Chem. C* **2021**, *125*, 5037.
[240] E. Ronge, J. Ohms, V. Roddatis, T. Jones, F. Sulzmann, A. Knop-Gericke, R. Schlögl, P. Kurz, C. Jooss, K. Skorupska, *Sustainable Energy Fuels* **2021**, *5*, 5535.

[241] P. Busse, Z. Yin, D. Mierwaldt, J. Scholz, B. Kressdorf, L. Glaser, P. S. Miedema, A. Rothkirch, J. Viefhaus, C. Jooss, S. Techert, M. Risch, *J. Phys. Chem. C* **2020**, *124*, 7893.
[242] P. Wernet, K. Kunnus, I. Josefsson, I. Rajkovic, W. Quevedo, M. Beye, S. Schreck, S. Grübel, M. Scholz, D. Nordlund, W. Zhang, R. W. Hartsock, W. F. Schlotter, J. J. Turner, B. Kennedy, F. Hennies, F. M. F. de Groot, K. J. Gaffney, S. Techert, M. Odelius, A. Föhlisch, *Nature* **2015**, *520*, 78.
[243] K. Kunnus, I. Josefsson, I. Rajkovic, S. Schreck, W. Quevedo, M. Beye, C. Weniger, S. Grübel, M. Scholz, D. Nordlund, W. Zhang, R. W. Hartsock, K. J. Gaffney, W. F. Schlotter, J. J. Turner, B. Kennedy, F. Hennies, F. M. F. de Groot, S. Techert, M. Odelius, P. Wernet, A. Föhlisch, *Struct. Dyn.* **2016**, *3*, 4.
[244] S. Schreck, A. Pietzsch, B. Kennedy, C. Sathe, P. S. Miedema, S. Techert, V. N. Strocov, T. Schmitt, F. Hennies, J.-E. Rubensson, A. Föhlisch, *Sci. Rep.* **2016**, *6*, 20054.
[245] J. Schlappa, G. Ghiringhelli, B. E. Van Kuiken, M. Teichmann, P. S. Miedema, J. T. Delitz, N. Gerasimova, S. Molodtsov, L. Adriano, B. Baranasic, C. Broers, R. Carley, P. Gessler, N. Ghodrati, D. Hickin, L. P. Hoang, M. Izquierdo, L. Mercadier, G. Mercurio, S. Parchenko, M. Stupar, Z. Yin, L. Martinelli, G. Merzoni, Y. Y. Peng, T. Reuss, S. S. N. Lalithambika, S. Techert, T. Laarmann, S. Huotari, et al., *arXiv:2403.08461[cond-mat.str-el]* **2024**.
[246] Z. Yin, H. B. Peters, U. Hahn, M. Agaker, A. Hage, R. Reininger, F. Siewert, J. Nordgren, J. Viefhaus, S. Techert, *Rev. Sci. Instrum.* **2015**, *86*, 9.
[247] F. Marschall, Z. Yin, J. Rehanek, M. Beye, F. Döring, K. Kubicek, D. Raiser, S. T. Veedu, J. Buck, A. Rothkirch, B. Rösner, V. A. Guzenko, J. Viefhaus, C. David, S. Techert, *Sci. Rep.* **2017**, *7*, 8849.
[248] Z. Yin, L. Inhester, S. Thekku Veedu, W. Quevedo, A. Pietzsch, P. Wernet, G. Groenhof, A. Föhlisch, H. Grubmüller, S. Techert, *J. Phys. Chem. Lett.* **2017**, *8*, 3759.

Christian Jooss is a professor at the Institute of Materials Physics, University of Göttingen, Germany since 2008. His main interests are to study new pathways of controlling energy conversion in strongly correlated material systems and the development of suitable in situ transmission electron microscopy methods. He is spokesperson of an interdisciplinary collaborative research center on "atomic-scale control of energy conversion" at the Göttingen campus.

Michael Seibt is currently a professor at Georg-August-University Göttingen, at the 4th Institute of Physics – Solid State and Nanostructures. He received his Doctoral Degree at the University of Göttingen in 1986 and worked at AT&T Bell Laboratories, US, in 1992–1993. His research interests are semiconductors, their defects and applications, and transmission electron microscopy.

Martin Wenderoth is currently a professor at Georg-August-University Göttingen. After completing his doctorate at the University of Göttingen, he headed the scanning probe microscopy working group at the 4th Institute of Physics – Solid State and Nanostructures. His area of expertise is the further development of scanning probe techniques with the aim of understanding electronic correlations in semiconductors and metals on the nanometer scale.

Oliver Bünermann received his Ph.D. from the University of Bielefeld in 2006. After postdoctoral stays at the University of Freiburg and University of California, Berkeley, he became group leader at the Institute of Physical Chemistry of the University of Goöttingen in 2010. In Goöttingen, he developed a new experiment to study inelastic scattering of H atoms from surfaces. His research interest is the interaction of H atoms with surfaces

Matthias Krüger is a professor in Theoretical Physics at Georg-August University of Göttingen. He received his Doctoral Degree at the University of Konstanz in 2009. Afterward, he was a postdoctoral fellow at Massachusetts Institute of Technology, Cambridge, USA. He is interested in the Statistical Physics of systems far from equilibrium.

Claus Ropers studies ultrafast nanoscale dynamics using imaging and diffraction with femtosecond electron and extreme-ultraviolet pulses. His group develops and applies Ultrafast Transmission Electron Microscopy (UTEM), Ultrafast Low-energy Electron Diffraction (ULEED), and Ultrafast High-harmonic Nanoscopy. Studying physics in Göttingen and Berkeley, he received a Ph.D. in Berlin for work at the Max Born Institute (2007). He was a professor of physics at the University of Göttingen from 2008 on, and in 2020, became director at the Max Planck Institute for Multidisciplinary Sciences in Göttingen. Awards for his research include two ERC grants, the Ernst-Ruska-Prize, and the Gottfried Wilhelm Leibniz Prize.

Kai Rossnagel is a professor of Experimental Physics at Kiel University and a Lead Scientist at the Deutsches Elektronen-Synchrotron DESY, Hamburg, Germany. He received his Ph.D. in physics from Kiel University in 2001, was a Feodor Lynen Research Fellow at the Advanced Light Source in Berkeley, USA, and spent several extended research stays as a visiting scientist at the RIKEN SPring-8 Center, Japan (2013–15). His research expresses his passion for growing transition-metal dichalcogenide crystals and understanding their properties and functions at the atomic level through their electronic structure and ultrafast dynamics.

Simone Techert is a leading scientist within the Photon Science division of the Deutsches Elektronen-Synchrotron DESY, Hamburg, and a professor for Ultrafast X-ray Science at Göttingen University. Her research concentrates on kinetic and time-resolved (ultrafast, in situ, *operando*) X-ray methods development for complex chemical systems and reaction studies (like water splitting or photovoltaics) and the investigation of the electronic and structural properties and dynamics of (sustainable) functional materials.

Cynthia Volkert is a professor at the Institute of Materials Physics at the University of Göttingen where she specializes in the mechanical behavior and stability of nanoscale materials and in situ electron microscopy. After a bachelor degree in physics from McGill University and a Ph.D. degree from Harvard University, she spent 10 years as a staff member at Bell Laboratories in New Jersey. She then moved to Germany where she focused on micro-mechanical and in situ testing methods first at the Max Planck Institute for Metals Research in Stuttgart and then at the Research Center Karlsruhe before moving to Göttingen in 2007.

R. Thomas Weitz received his diploma in physics at the University of Heidelberg and his Ph.D. from the Max-Planck-Institute for Solid State Physics in Stuttgart. After a PostDoc at Harvard University and the MPI in Stuttgart, he went into industrial research at BASF SE, Ludwigshafen. After having been a professor at the Ludwig-Maximilians University, Munich he is currently a full professor at the 1st Institute of Physics at the Georg August University of Göttingen. His research is focused on quantum transport in low-dimensional materials, organic electronics, and energy conversion at the nanoscale.

Alec Wodtke is an experimentalist studying chemical reaction dynamics. As a professor at UCSB, he developed methods for observing collision dynamics of highly vibrationally excited molecules. This produced results on topics from the quantum nature of chemical isomerization to the role of hot molecules in stratospheric ozone production. In 2010, he was awarded a Humboldt Professorship and became a Max Planck Director and University Professor in Germany. He now studies fundamental problems in surface chemistry emphasizing interactions between experiment and theory, work that was rewarded with an ERC Advanced Grant Award in 2017 and the Gerhard Ertl Lecture Award in 2022.